Palmitoylation-dependent activation of MC1R prevents melanomagenesis

HHS Public Access

Author manuscript

Nature. Author manuscript; available in PMC 2018 April 17.

Published in final edited form as:

Nature. 2017 September 21; 549(7672): 399–403. doi:10.1038/nature23887.

Palmitoylation-dependent activation of MC1R prevents melanomagenesis

Shuyang Chen[1,10], **Bo Zhu**[1,10], **Chengqian Yin**[1,10], **Wei Liu**[1], **Changpeng Han**[1], **Baoen Chen**[2], **Tongzheng Liu**[3], **Xin Li**[1], **Xiang Chen**[4], **Chunying Li**[5], **Limin Hu**[6], **Jun Zhou**[7], **Zhi-Xiang Xu**[8], **Xiumei Gao**[6], **Xu Wu**[2], **Colin R. Goding**[9], and **Rutao Cui**[1,*]

[1]Department of Pharmacology and Experimental Therapeutics, Boston University School of Medicine, Boston, MA 02118, USA

[2]Cutaneous Biology Research Center, Massachusetts General Hospital, Harvard Medical School, Charlestown, MA 02129, USA

[3]Jinan University Institute of Tumor Pharmacology, Guangzhou, Guangdong, 510632, China

[4]Hunan key Laboratory of Skin Cancer and Psoriasis/Department of Dermatology, Xiangya Hospital, Central South University, Changsha, Hunan, 410008, China

[5]Department of Dermatology, Xijing Hospital, The Fourth Military Medical University, Xi'an, Shaanxi, 710000, China

[6]Tianjin State Key Laboratory of Modern Chinese Medicine, Tianjin University of Traditional Chinese Medicine, Tianjin, 300193, China

[7]State Key Laboratory of Medicinal Chemical Biology, College of Life Sciences, Nankai University, Tianjin 300071, China

[8]Division of Hematology and Oncology, Department of Medicine, Comprehensive Cancer Center, University of Alabama at Birmingham, Birmingham, AL 35294, USA

[9]Ludwig Institute for Cancer Research, University of Oxford, Headington, Oxford, OX3 7DQ, UK

Abstract

*To whom correspondence should be addressed: Rutao Cui: rutaocui@bu.edu.
[10]These authors contributed equally to this work.

Supplementary Information is in available in the online version of the paper.

Author Contributions R.C. conceived the hypothesis, organized and supervised the study. R.C. designed the project with help from S.C., B.Z. and C.Y. S.C., B.Z. and C.Y. analyzed and interpreted data. S.C. performed mouse experiments (e.g., melanoma free survival, histopathology) with assistance from C.Y. B.Z. independently reproduced mouse experiments with assistance from W.L. and C.H. S.C. performed protein palmitoylation assay. B.Z. and C.Y. independently reproduced protein palmitoylation assay with assistance from W.L. and C.H. S.C. performed melanocytes function (e.g., cAMP, MITF, DNA repair, senescence) measurement and cellular transformation assay, which were independently reproduced by C.Y. B.C. and X.W. designed and performed the transfection of HA-tagged ZDHHCs, which was independently reproduced by S.C. and C.Y. T.L., X.L., X.C., C.L., L.H., J.Z., Z.X., X.G., C.R.G. contributed to data analysis, interpretation and revision of the manuscript. R.C. wrote the manuscript with help from C.R.G. All authors commented on the manuscript.

The authors declare no competing financial interests.

The melanocortin-1 receptor (MC1R), a G protein-coupled receptor, plays a crucial role in human and mouse pigmentation[1–8]. Activation of MC1R in melanocytes by α-melanocyte-stimulating hormone (α-MSH)[9] stimulates cAMP signaling and melanin production and enhances DNA repair after UV irradiation (UVR)[10–16]. Individuals carrying MC1R variants, especially those associated with red hair color, fair skin and poor tanning ability (RHC-variants), are associated with higher risk of melanoma[5,17,18,19,20]. However, how MC1R activity might be modulated by UV irradiation, why redheads are more prone to developing melanoma, and whether the activity of RHC variants might be restored for therapeutic benefit remain unresolved questions. Here we demonstrate a potential MC1R-targeted intervention strategy to rescue loss-of-function MC1R in *MC1R* RHC-variants for therapeutic benefit based on activating MC1R protein palmitoylation. Specifically, MC1R palmitoylation, primarily mediated by the protein-acyl transferase (PAT) ZDHHC13, is essential for activating MC1R signaling that triggers increased pigmentation, UVB-induced G1-like cell cycle arrest and control of senescence and melanomagenesis *in vitro* and *in vivo*. Using C57BL/6J-*MC1R*$^{e/e}$J mice expressing *MC1R* RHC-variants we show that pharmacological activation of palmitoylation rescues the defects of *MC1R* RHC-variants and prevents melanomagenesis. The results highlight a central role for MC1R palmitoylation in pigmentation and protection against melanoma.

A preliminary small molecule screen to identify novel modulators of RHC-variant MC1R activity suggested that palmitic acid increased cAMP levels in human primary melanocytes with an endogenous MC1R R151C variant (HPM-RHC), or engineered RHC-variant B16 melanoma cells (B16-RHC) in which MC1R R151C was reintroduced after deletion of the endogenous gene (MC1R reconstituted cells). To validate this result, HPM-RHC and B16-RHC were serum starved, pretreated with α-MSH and exposed to one standard erythema dose of UVB (100 J/m^2), before being treated with medium containing BSA-conjugated fatty acids for 3 h. Palmitic acid, but not other lipids, increased cAMP levels in both HPM-RHC and B16-RHC (Fig. 1a, Extended Data Fig. 1a).

Since palmitic acid can induce palmitoylation of cysteine residues (Extended Data Fig. 1b) we treated cells with the general palmitoylation inhibitor 2-BP (2-bromopalmitate). 2-BP prevented palmitic acid-induced cAMP levels in both HPM-RHC and B16-RHC (Fig. 1b, Extended Data Fig. 1c) as well as in WT B16 and HPMs, with the effect of palmitic acid being dependent on α-MSH and stimulated by UV irradiation (Extended Data Fig. 1d-e). Using an acyl-biotin exchange (ABE) assay in HPM-RHCs (Extended Data Fig. 1f), free cysteine thiol groups were irreversibly blocked by N-Ethylmaleimide (NEM), palmitoylated cysteines exposed by hydroxylamine (HAM) and biotinylated. Labeled proteins pulled down using streptavidin-dynabeads were analyzed by mass spectrometry (MS) (Extended Data Fig. 1g) to reveal that MC1R is palmitoylated (Extended Data Fig. 1h), consistent with integral membrane proteins G protein-coupled receptors (GPCRs) like MC1R[9] being palmitoylated during activation. Palmitoylation site prediction (NBA-palm) analysis[21] highlighted MC1R Cysteines 78 and 315 as potential palmitoylation sites (Extended Data Fig. 1i-k).

Palmitoylation of both endogenous MC1R and exogenously expressed Flag-MC1R was confirmed using streptavidin to detect MC1R protein labeled using ABE following

immunoprecipitation from B16 and HPMs stimulated with α-MSH (Fig. 1c-d, Extended Data Fig. 2a-b). The Flag-MC1R C78S mutant but not Flag-MC1R C315S was also palmitoylated (Fig. 1e, Extended Data Fig. 2c), indicating that C315 is the major MC1R palmitoylation site.

Using MC1R reconstituted cells, in the presence of α-MSH both R151C and R160W MC1R variants exhibited reduced palmitoylation compared to WT (Fig. 1f, Extended Data Fig. 2d). Moreover, a C315S mutation in the context of the R151C variant completely blocked MC1R R151C palmitoylation, indicating Cys151 is not a neo-palmitoylation site (Extended Data Fig. 2e-f). Notably UVR-stimulated palmitoylation of endogenous MC1R and exogenously expressed Flag-MC1R (Fig. 1g-h, Extended Data Fig. 2g-h), but not the MC1R C315S mutant (Fig.1i, Extended Data Fig. 2i), whereas UVR-induced palmitoylation of the R151C and R160W RHC-variants was reduced compared to the WT protein (Fig. 1j-k and Extended Data Fig. 2j-m).

To identify which protein *S*-acyl transferases (PATs) were responsible for MC1R modification, 23 HA-tagged ZDHHC PATs[22] were co-expressed with Flag-MC1R. Detectable MC1R palmitoylation was only observed following expression of ZDHHC2, 3, 7, 13 and 17 (Extended Data Fig. 3a), with ZDHHC13 the most efficient (Fig. 2a). MC1R palmitoylation was substantially reduced in cells expressing a C456S mutant ZDHHC13 in which the enzymatic DQHC motif was mutated (Fig. 2b, Extended Data Fig. 3b). Silencing ZDHHC13 diminished UVR-stimulated palmitoylation of WT MC1R (Fig. 2c, Extended Data Fig. 3c), as well as the R151C RHC variant (Fig. 2d, Extended Data Fig. 3d), whereas ZDHHC13 overexpression activated MC1R R151C palmitoylation (Fig. 2d, Extended Data Fig. 3d-f). The MC1R C315S mutant was used as a negative control.

Interaction between ZDHHC13 and MC1R was detected by co-immunoprecipitation from α-MSH-treated HPMs and was enhanced by UVR (Fig. 2e), reflecting increased MC1R palmitoylation following UVR (Extended Data Fig. 3g-h). Interaction between the MC1R RHC R151C and R160W proteins and ZDHHC13 was also increased after UVR, but was much less than with WT MC1R (Fig. 2f).

Since ATR is a central effector of the UVB-response[23,24] we asked if ATR-mediated phosphorylation of ZDHHC13 promoted MC1R palmitoylation following UV exposure. HPMs expressing HA-ZDHHC13 were irradiated with UVB and after anti-HA immunoprecipitation phosphorylation of ZDHHC13 was detected by with specific phospho-S/T-Q antibody. The results revealed UVB treatment increased ZDHHC13 phosphorylation (Fig. 2g) and MC1R-ZDHHC13 interaction (Fig. 2h) that was substantially reduced in cells stably expressing shATR (Fig. 2i). Mutation of an evolutionarily conserved SQ site at Ser8 (Extended Data Fig. 3i) prevented UVR-stimulated ZDHHC13 phosphorylation (Extended Data Fig. 3j) and ATR WT, but not a kinase-dead mutant, robustly phosphorylated recombinant WT ZDHHC13, but not the S8A mutant (Extended Data Fig. 3k). Compared to WT ZDHHC13, the S8A mutant only weakly interacted with MC1R (Extended Data Fig. 3l) and failed to enhance MC1R palmitoylation upon UVB irradiation (Extended Data Fig. 3m). Collectively these results suggest that ZDHHC13 phosphorylation by ATR following UVB irradiation promotes its interaction with MC1R to stimulate MC1R palmitoylation.

To test whether MC1R palmitoylation regulates MC1R signaling[10–16] cAMP levels were measured after UVB irradiation and α-MSH stimulation of MC1R reconstituted cells. Whereas WT MC1R significantly increased cAMP levels following UVR, the palmitoylation-deficient mutant C315S failed to do so, and RHC variants partially lost their ability to stimulate cAMP production (Extended Data Fig. 4a). The C315S mutant also failed to up-regulate microphthalmia-associated transcription factor (MITF) and tyrosinase (TYR) mRNA expression (Extended Data Fig. 4b-c) downstream from MC1R signaling. The MC1R RHC variants only weakly activated MITF and TYR expression compared to WT, strongly suggesting that palmitoylation is essential for MC1R signaling.

To examine the role of MC1R palmitoylation in α-MSH/MC1R-regulated DNA repair, endogenous MC1R reconstituted HPMs and cyclobutane pyrimidine dimer (CPD) and 6-4 photoproducts (6-4 PPs) were measured following UVB exposure. Although WT MC1R promoted photoproduct clearance, the palmitoylation-defective C315S mutant, or the RHC variants failed to repair the lesions efficiently (Extended Data Fig. 4d).

Consistent with previous work[25] silencing MC1R augments low dose UVB-induced premature senescence that was bypassed by reintroduction of WT MC1R (Extended Data Fig. 4e). The R151C and R160W RHC variants also exhibited a defective senescence bypass phenotype whereas the C315S mutant was ineffective (Extended Data Fig. 4f). Using engineered human immortal melanocytes (hTERT/p53DD/CDK4(R24C) melanocytes)[25,26] in colony formation and soft agar growth assays we found that $BRAF^{V600E}$-mediated cellular transformation was suppressed by WT MC1R, but not the C315S mutant, while the R151C and R160W variants exhibited an intermediate phenotype (Fig. 3a, Extended Data Fig. 4g-k).

To examine its role in cAMP production, ZDHHC13 was silenced or overexpressed in MC1R reconstituted B16 cells and HPMs, and cAMP levels measured following UVB irradiation and α-MSH stimulation. ZDHHC13 overexpression increased cAMP levels in cells expressing WT MC1R and also rescued the defect in cAMP production in cells expressing the R151C variant (Extended Data Fig. 5a). ZDHHC13 overexpression increased MITF expression in WT cells and rescued the defect in α-MSH/MC1R RHC variant-induced MITF up-regulation (Extended Data Fig. 5b). The palmitoylation defective C315S mutant was inactive irrespective of ZDHHC13 expression. ZDHHC13 overexpression enhanced UVR-induced DNA damage repair and rescued the defect in photoproduct clearance in melanocytes with the MC1R R151C variant, whereas ZDHHC13 depletion impaired repair (Extended Data Fig. 5c). Similarly, ZDHHC13 overexpression protected against UVB-induced premature senescence in melanocytes expressing WT and R151C MC1R, but not those expressing the C315S mutant, whereas shRNA depletion of ZDHHC13 enhanced senescence in cells expressing WT or R151C MC1R (Extended Data Fig. 5d).

Soft agar and colony formation assays using the human hTERT/p53DD/CDK4(R24C) melanocytes[25,26] revealed that ZDHHC13 depletion increased transformation by $BRAF^{V600E}$ in the presence of WT MC1R, whereas enhanced transformation by the R151C mutant was suppressed by ZDHHC13 overexpression (Fig. 3b, Extended Data Fig. 5e). Elevated transformation in the presence of the C315S mutant was unaffected by ZDHHC13

overexpression/depletion. Subcutaneous xenograft tumor assays also indicated that ZDHHC13 overexpression inhibits MC1R R151C-augmented $BRAF^{V600E}$–induced malignant transformation (Fig. 3c-e).

We next used MC1R loss-of-function (C57BL/6J-*MC1R*$^{e/e}$J) mice, backcrossed to C57BL/6 for more than 24 generations, to generate transgenics re-expressing melanocyte-specific WT, RHC variant and C315S mutant MC1R (Extended Data Fig. 6a). Unlike previous transgenic MC1R RHC mice developed by Healy et al[3] using bacterial artificial chromosomes (BAC), our $MC1R^{R151C}$ variant offspring show a mosaic coat color that could arise as a consequence of the promoter used, integration site, or mouse strain background. Our other RHC-variants exhibited a paler coat color than WT (Fig. 4a, Extended Data Fig. 6b). All mice are at generation F26 or later with stable fur phenotypes and exhibit similar expression levels of the human transgenic MC1R mRNAs (Extended Data Fig. 6c). The MC1R R151C variant mice also exhibit higher skin pheomelanin/eumelanin ratios than WT mice (Fig. 4b). Strikingly, the palmitoylation-deficient MC1R C315S-espressing mice showed a similar coat color and skin pheomelanin content to the C57BL/6J-*MC1R*$^{e/e}$J mice (Fig. 4b, Extended Data Fig. 6b), with no significant difference in number/distribution/location of melanocytes detected in mice with $MC1R^{+/+}$, $MC1R^{e/e}$, $MC1R^{R151C}$ and $MC1R^{C315S}$ (Extended Data Fig. 6d-e).

Tyr-Cre-$BRAF^{CA}$ mice (B6.Cg-*Braf*^{tm1Mmcm} Tg(Tyr-cre/ERT2)13Bos/BosJ)[27] were next crossed to the $MC1R^{e/e}$, $MC1R^{+/+}$, $MC1R^{R151C}$ and $MC1R^{C315S}$ mice and $BRAF^{V600E}$ expression induced by tamoxifen administration. After UVB irradiation each week for four weeks (Extended Data Fig. 5f) melanomas developed early and frequently in MC1R loss-of-function (e/e) or palmitoylation-defective MC1R transgenic (C315S) mice, much later with WT MC1R mice, and at an intermediate time with the MC1R R151C variant (Fig. 4c). All melanomas diagnosed displayed similar morphological and histologic features (Extended Data Fig. 6g).

To explore whether MC1R palmitoylation is dynamic, we removed α-MSH from the culture medium and found that palmitoylation disappeared within 12 h, while Palm-B, a deacylating enzyme inhibitor[28,29], blocked both WT and R151C MC1R depalmitoylation (Extended Data Fig. 7a), suggesting that Palm-B enhances MC1R palmitoylation. Treatment of endogenous MC1R reconstituted B16 cells with Palm-B, together with α-MSH and UVB irradiation, increased MC1R R151C palmitoylation to levels detected for the WT protein, whereas no palmitoylation was observed using the C315S mutant irrespective of Palm-B administration (Extended Data Fig. 7b). Using HPMs or B16 cells reconstituted with WT or variant MC1R, Palm-B moderately increased α-MSH-induced cAMP production, but dramatically increased signaling from the R151C variant to levels comparable to those observed from α-MSH-stimulated WT MC1R in the absence of Palm-B (Extended Data Fig. 7c). Signaling downstream from the R151C variant, as well as WT MC1R, was functional since both MITF and TYR mRNA expression were upregulated by Palm-B (Extended Data Fig. 7d-e). Palm-B also accelerated clearance of UVR-induced photoproducts in melanocytes with the MC1R R151C variant (Extended Data Fig. 7f). By performing ABE on extracts from mouse skin irradiated with UVB we confirmed that Palm-B administration to mice increased MC1R palmitoylation in $MC1R^{R151C}$ and $MC1R^{+/+}$ *in vivo* (Extended

Data Fig. 7g). Following UVB treatment, both CPD and 6-4pp DNA lesions were significantly higher in R151C mice than in WT mice, with Palm-B reducing the levels of damage detected in both (Extended Data Fig. 7h-i). Notably, Palm-B also repressed low-dose UVB-induced premature senescence in HPMs or B16 cells reconstituted with the MC1R R151C variant (Extended Data Fig. 7j). Using human immortal hTERT/p53DD/CDK4(R24C) melanocytes Palm-B largely reversed the increased colony formation observed using the R151C variant (Fig. 4d, Extended Data Fig. 7k) and in xenograft studies, Palm-B inhibited MC1R R151C-augmented $BRAF^{V600E}$ melanomagenesis (Fig. 4e-g). Importantly, Palm-B had no effect in any assay using the C315S mutant.

Finally, to confirm the preventive effect of Palm-B in melanomagenesis in redheads, Tyr-Cre-$BRAF^{CA}$-$MC1R^{e/e}$-$MC1R^{R151C}$ mice were UVB irradiated each week for four weeks, with 10 mg/kg Palm-B injected intraperitoneally into Tyr-Cre-$BRAF^{CA}$-$MC1R^{e/e}$-$MC1R^{R151C}$ mice prior to the treatment with UV. While no strong side effects were observed, in Palm-B treated mice melanomagenesis was substantially delayed and the incidence reduced (Fig. 4h). Similar results were obtained using Palm-B and the MC1R R160W variant (Extended Data Fig. 8). Collectively our results highlight a central role for MC1R palmitoylation in protecting against melanoma, and suggest that rescuing MC1R palmitoylation by up-regulation of ZDHHC13 or inhibition of depalmitoylation might be a potential clinical prevention strategy for melanoma in redheads.

Methods

Cell Lines, Animals and UV Exposure

Cell lines and UV exposure were as described previously[2,25,30]. All cell lines were authenticated and mycoplasma negative. Briefly, cells were washed by PBS twice before UVB irradiation. For the *in vitro* UV experiments, cells were exposed to ultraviolet radiation in the Stratalinker UV chamber (Stratagene, Cedar Creek, TX, USA) with UVB bulbs (UVP LLC, Upland, CA, USA). UV emittance was measured with the use of a UV photometer (UVP LLC, Upland, CA, USA)[30]. Adherent cells were irradiated through a small volume of PBS at a dose of 100 J/m^2. A UVB dose of 100 J/m^2 is equivalent to one standard erythema dose of UVB (SED), commonly used as a measurement of sunlight. As a reference, the ambient exposure over an entire sunny summer day in Europe (Switzerland) is approximately 30-40 SED[31]. Human primary melanocytes were isolated from normal discarded foreskins as described before[32,33] and were cultured in Medium 254 (Thermo Fisher Scientific Inc., Waltham, MA, USA). In all assays, cells were pretreated with α-MSH (1 μM) for 30 min following with 100 J/m^2 UVB irradiation, and collected 3 h after UVB exposure. Palm B was used at 1 μM.

The maximal tumor size is 20 mm at the largest diameter, which was permitted by IACUC of Boston University Medical Campus. None of the experiments exceeded the limit. Mice were maintained in specific-pathogen-free facility of Animal Science Center (ASC) of Boston University Medical Campus, and the experiments were performed according to the Institutional Animal Care and Use Committee of Boston University Medical Campus. Mice were housed on a time cycle of 12 h of light (beginning at 6:00 AM) and 12 h of dark (beginning at 6:00 PM). Mice were allowed free access to an irradiated diet and sterilized

water. The mice were monitored daily for signs of health status and distress. Mice with age from 8 weeks to 6 months were used for breeding and pregnant female will be placed in a new cage. Mice were weaned at 20 - 21 days of age. DNA was extracted from the mouse tail biopsy for genotyping. NCr nude mice (female, 8-10 weeks) were purchased from Taconic Biosciences. C57BL/6J-*MC1R*$^{e/e}$J (The Jackson Laboratory, Stock No: 000060) homozygous mice were crossed with Tyr-Cre-BRAF^{CA} mice (B6.Cg-*Braf*^{tm1Mmcm} Tg(Tyr-cre/ERT2)13Bos/BosJ) (The Jackson Laboratory, Stock No: 017837) homozygous mice to generate Tyr-Cre-BRAF^{CA}-*MC1R*$^{+/e}$ heterozygous mice, which were crossed to generate the age-matched C57BL/6J-Tyr-Cre-BRAF^{CA}-*MC1R*$^{+/+}$ mice and C57BL/6J-Tyr-Cre-BRAF^{CA}-*MC1R*$^{e/e}$ for experiments. All these mice are genotyped according to The Jackson Laboratory's protocol. All mice are with stable fur phenotypes at generation F26 or later.

Transgenic mice were designed to express melanocyte-specific MC1R RHC-variant (controlled by the Tyr enhancer/promoter) and generated by Boston University School of Medicine Transgenic and Genome Engineering Core. The expression construct was designed such that the MC1R gene was inserted downstream of the murine tyrosinase locus control region. Each construct was injected into single-cell embryos of C57BL/6J-*MC1R*$^{e/e}$J mice. The transgene was detected by genotyping mice tail DNA using the primers targeting fragment across Tyr promoter and MC1R region (~1200 bp, forward 5′-GGGCTATGTACAAACTCCAAGA′-3, reverse 5′-ACACTTAAAGCGCGTGCACCGC-′3). The expression levels of human transgene were determined as described[3]. Briefly, total RNA was collected from primary melanocytes isolated from neonatal transgenic mouse skins using RNeasy Mini Kit (Qiagen, Hilden, Germany). A sequential DNA remove was performed by DNA-free™ DNA Removal Kit (Thermo Fisher Scientific Inc., Waltham, MA, USA) to avoid genomic DNA contamination. Reverse transcription was carried out with random primers. Primers were used as previously described[7] to amplify both the mouse and human MC1R. A following extension was performed using primer as previously described[3] by adding ddTTP (mouse MC1R) or ddCTP (human MC1R) (SNaPshot Multiplex Kit, Thermo Fisher Scientific Inc.). Extension products were separated by capillary electrophoresis and quantified by measuring human/mouse MC1R ratio. Mice underwent tamoxifen treatment to express BRAF^{V600E} in melanocytes. Briefly, mice at 3 weeks of age were administered with tamoxifen (T5648) (Sigma-Aldrich, St. Louis, MO, USA) in corn oil daily by intraperitoneal injection at 0.12 mg/g body weight for 5 consecutive days. The control mice will get plain corn oil injection. Mouse UV exposure procedure was performed as described previously[30]. Briefly, a UVB dose of 500 J/m^2 was used. This does is equivalent to one minimum erythema dose of UVB (MED) and 5 standard erythema doses of UVB (SED), commonly used as a measurement of sunlight *in vivo*.

Plasmid, Transfection, Lentiviral and Retroviral Infections

23 HA-tagged ZDHHC family protein-encoding plasmids are provided by Dr. Xu Wu with the permission of Dr. Fukata[22]. pcDNA3-Flag-MC1R WT and RHC variants R151C, R160W and D294H were generated as previously described[25]. To generate the MC1R or ZDHHC13 expression plasmids for retroviral infection, the cDNAs were subcloned into pQCXIP (Clonetech) at the NotI/EcoRI sites, respectively. All other mutants were generated by site-directed mutagenesis using the QuickChange II Site-Directed Mutagenesis kit

(Agilent, Santa Clara, CA, USA). To generate stable knockdown of MC1R or ZDHHC13 in B16 and HPMs, mouse or human specific short hairpin RNAs in pLKO.1 against MC1R or ZDHHC13 were co-transfected with psPAX2 (Addgene #12260) and pMD2.G (Addgene, #12259) in HEK293-FT (ATCC) using Lipofectamine 3000 (Thermo Fisher Scientific Inc., Waltham, MA, USA). Lentiviruses were collected after 48 h, and then infected cells for 24 h in the presence of polybrene (8 μg/mL) and the infected cells were selected with puromycine (2 μg/mL). To generate cells with stable expression of MC1R variants or HA-ZDHHC13, HEK293T cells were co-transfected with MC1R variants or HA-ZDHHC13 in pQCXIP, VSV-G and pUMVC (Addgene #8449) plasmids using Lipofectamine 3000. Retroviruses were harvested after 48 h and cells were infected with retroviruses in the presence of polybrene (8 μg/mL). After 24 h, cells were selected with puromycine (2 μg/mL). shRNA constructs targeting human MC1R (RHS4533-EG4157), mouse MC1R (RMM4534-EG17199), human ZDHHC13 (RHS4533-EG54503), mouse ZDHHC13 (RMM4534-EG243983) and human ATR (RHS4533-EG545) were purchased from OpenBiosystems. The most efficient knockdown cell lines with shmMC1R (target sequence: 5′-AATGGAGATCAGGAAGGGATG-3′) or shMC1R (target sequence: 5′-AAATGTCTCTTTAGGAGCCTG-3′) were used in assays. pcDNA3-ATR WT (addgene #31611) and pcDNA3-ATR Kinase dead (addgene #31612) were gifts from Aziz Sancar[34].

Immunoblot Analysis

High Sensitivity Streptavidin-HRP (21130) and Dynabeads® MyOne™ Streptavidin C1 (65001) were purchased from Thermo Fisher Scientific Inc. Anti-ZDHHC13 antibody (ab28759) was purchased from Abcam. Anti-MC1R antibody (N-19) (sc-6875) was purchased from Santa Cruz Biotechnologies, Inc. Monoclonal Anti-β-Actin−Peroxidase antibody (AC15), monoclonal Anti-FLAG® M2-Peroxidase antibody (A8592), Monoclonal Anti-HA−Peroxidase antibody (H6533), anti-Flag agarose beads (A2220), anti-HA agarose beads (A2095), peroxidase-conjugated anti-mouse secondary antibody (A4416) and peroxidase-conjugated anti-rabbit secondary antibody (A-4914) were purchased from Sigma-Aldrich. All western blot shown are representatives of three independent experiments.

Co-immunoprecipitation

Briefly, Cells were washed twice with ice-cold phosphate-buffered saline and lysed in lysis buffer containing 50 mM Tris pH 7.4; 1% Triton X-100; 0.5 mM EDTA; 0.5 mM EGTA; 150 mM NaCl; 10% Glycerol; 1 mM phenylmethylsulfonyl fluoride, complete protease inhibitor cocktail (Roche) on ice for 30 min. The supernatant was collected after centrifugation at 15,000 × g for 15 min at 4 °C, and 500 μg of total cell lysate was treated by DNase (15 U/mL, Pierce), precleared by 20 μl Protein G Agarose Beads (Thermo Fisher Scientific Inc.) and then incubated with primary antibodies overnight at 4 °C or Flag/HA beads (Sigma-Aldrich) directly for 2 h. 20 μl of Protein G Agarose Beads was added into the samples with rotation at 4 °C for 1 h. After three washes with 1 mL of lysis buffer, the bound proteins were released by boiling in 30 μL of SDS loading buffer and detected as described above.

Acyl-biotin exchange palmitoylation assay

Briefly, cells were lysed by lysis buffer (1% IGEPAL CA-630, 50mM Tris-HCl, pH7.5, 150mM NaCl 10% Glycerol and protease inhibitor) with 50 mM N-Ethylmaleimide (NEM) (Sigma-Aldrich) and endogenous MC1R or Flag-MC1R is then purified by specific antibodies and beads. Purified MC1R protein were divided into two groups, and one treated with lysis buffer + 1 M hydroxylamine (HAM) (Sigma-Aldrich) for 1 hr at room temperature. Finally, the beads were gently washed by lysis buffer pH 6.2 and incubated with lysis buffer pH 6.2 + 2 μM Biotin-BMCC (Thermo Fisher Scientific Inc.) for 1 hr at 4 °C. Proteins were washed 3 times and proceeded for IB analysis.

Mass Spectrometry

Mass spectrometry protein identification was performed by the Taplin Biological Mass Spectrometry Facility, Harvard Medical School. Protein samples were mixed with sample buffer and heated at 100 ℃ for 5 min, then loaded to SDS-PAGE for separation. When running was finished, gel was immersed within staining solution (0.3 % Coomassie Brilliant Blue, 45 % Methanol, 10 % Glacial acetic acid and 45 % dH_2O) and placed on shaker for 30 min. Gel was destained in destaining solution (20% Methanol, 10% Glacial acetic acid, 70% dH_2O) on shaker for overnight. Finally, bands on gel were excised and sent to Taplin Biological Mass Spectrometry Facility for mass spectrometry protein identification.

Immunoassay

DNA damage immunoassay was performed using the anti-CPD (MC-062) and anti-6-4 PPs (KTM-50) antibodies. Briefly, the heat-denatured genomic DNA were coated onto the microplate wells with Pierce DNA Coating Solution (17250) (Thermo Fisher Scientific Inc., Waltham, MA, USA). After washing and blocking by PBS with the purified anti-mouse IgG mAb of 2 μg/mL, the specific antibodies of anti-CPD (MC-062) and anti-6-4 PPs (KTM-50) were diluted 1:1000 in blocking buffer and added to each well. Optical density at 405 nm was determined. Intracellular cAMP levels were measured by cAMP Direct Immunoassay Kit (ab65355) (Abcam, Cambridge, MA, USA) following manufacture's protocols, optical density at 450 nm was determined. For cAMP measurement with fatty acid treatment, fatty acids were dissolved in 100% ethanol (250 mM) mixed with 25 mM BSA and added to serum-free DMEM/medium 254 at a final concentration of 500 μM. Cells were serum starved for 6 h. For the last 30 min cells were incubated with 1 μM α-MSH, followed by 100 J/m^2 UVB treatment. Lastly cells were treated with indicated BSA-conjugated fatty acid medium for 3 h with or without 2-BP (25 μM). All results are calculated by three independent experiments.

Real-Time qPCR

The cDNA (40 ng) was used for quantitative PCR amplification with SYBR green PCR master mix (Thermo Fisher Scientific Inc., Waltham, MA, USA). The relative levels of expression of genes were normalized according to those of GAPDH. Quantitative real-time PCR (qRT-PCR) data were calculated using the comparative Ct method. All quantitative PCR were performed in triplicates, and three independent RNA samples were assayed for

each time point. All primers are listed and purchased from Integrated DNA Technologies (Coralville, IA, USA).

Mouse MITF forward GCCTGAAACCTTGCTATGCTGGAA, reverse AAGGTACTGCTTTACCTGGTGCCT.

Human MITF forward CGAGCTCATGGACTTTCCCTT A, reverse CTTGATGATCCGATTCACCAAA.

Mouse TYR forward ATTGATTTTGCCCATGAAGC, reverse CCCAGATCCTTGGATGTTATG.

Human TYR forward AGCACCCCACAAATCCTAACTTAC, reverse ATGGCTGTTGTACTCCTCCAATC.

Mouse GAPDH forward CCCATCACCATCTTCCAGGAGC, reverse CCAGTGAGCTTCCCGTTCAGC.

Human GAPDH forward ACCCACTCCTCCACCTTTGA, reverse CTGTTGCTGTAGCCAAATTCGT.

All results are calculated by three independent experiments.

Immunohistochemistry

Mouse melanomas were fixed in 10% formalin solution at 4°C overnight, paraffin-embedded and then cut in 5 μm-thick sections (Dermpath core facility, Boston University). Sections were then deparaffinized, rehydrated, and stained with anti-S-100 (Dako North America, Inc. Carpinteria, CA, USA) and counterstained with hematoxylin. Briefly, for antigen retrieval, sections were heated in a boiling water bath in 10 mM sodium citrate buffer (pH 6.0) for 20 min prior to immunostaining. Nonspecific staining was blocked by pre-incubation with Tris Buffered Saline (TBS)/0.1% Tween-20/5% normal goat serum (Jackson ImmunoResearch) for 1 h at room temperature. Tissue sections were incubated with the primary antibodies at 4°C overnight, and were subsequently incubated with secondary antibodies and detected with DAB substrate (Dako EnVision + System HRP, Dako) following manufacturer's instructions. Coverslips were mounted onto glass slides with permanent mounting medium. All images were taken with Olympus Inverted microscope (Cellular imaging core, Boston University).

Pigment measurement

Eumelanin were and pheomelanin were quantified by HPLC based on the level of pyrrole-2,3,5-tricarboxylic acid (PTCA) by alkaline hydrogen peroxide oxidation of eumelanin and 4-amino-3-hydroxyphenylalanine (4-AHP) by hydriodic acid reductive hydrolysis of pheomelanin, respectively. Final results were determined by a conversion as described (eumelanin=45×PTCA, peomelanin=9×4-AHP)[35]. All results are calculated by three independent experiments.

Clonogenic Survival and Soft Agar Assays

The clonogenic survival and soft agar assays for hTERT/p53DD/CDK4(R24C)/BRAF^{V600E} melanocytes were performed as described previously[26]. Briefly, for the melanocyte growth

promoting withdrawal experiments, hTERT/p53DD/CDK4(R24C)/BRAF^{V600E} melanocytes were treated with 20 J/m^2 UVB in the presence of 1 μM α-MSH before plating into 6-well plate at 1,000 cells per well, and then subject to clonogenic survival assays 15 days after UVR. Crystal violet was used to stain colonies. DMEM media was used with 10% FBS and penicillin/streptomycin/glutamine. For soft agar assays, cells (10,000 per well) were seeded in 0.5% low-melting-point agarose in DMEM with 10% FBS, layered onto 0.8% agarose in DMEM/10% FBS. The plates were kept in the cell culture incubator for 30 days after which the colonies >50 μm were counted under a light microscope. All results are calculated by three independent experiments.

In vivo Tumorigenesis Assay

In vivo tumorigenesis assay of hTERT/p53DD/CDK4(R24C)/BRAF^{V600E} melanocytes was performed as described previously[26]. Briefly, 3×10^6 melanocytes were mixed with matrigel (1:1) and injected subcutaneously into the flanks of male nude mice. Tumor size was measured every 3 days with a caliper, and the tumor volume was determined. Three weeks after inoculation, the tumors were dissected to measure their weights.

Statistical Analyses

All quantitative data were presented as the mean ± SD or ± SEM of at least three independent experiments by Student's t test for between group differences and analysis of variance for comparisons among three or more groups (*$p<0.05$, **$p<0.01$, ***$p<0.001$).

Data availability statements

All data that support the findings of this study are available on reasonable request from the corresponding author R.C. The contribution authors declare that all relevant data are included in the paper and its supplementary information files.

Extended Data

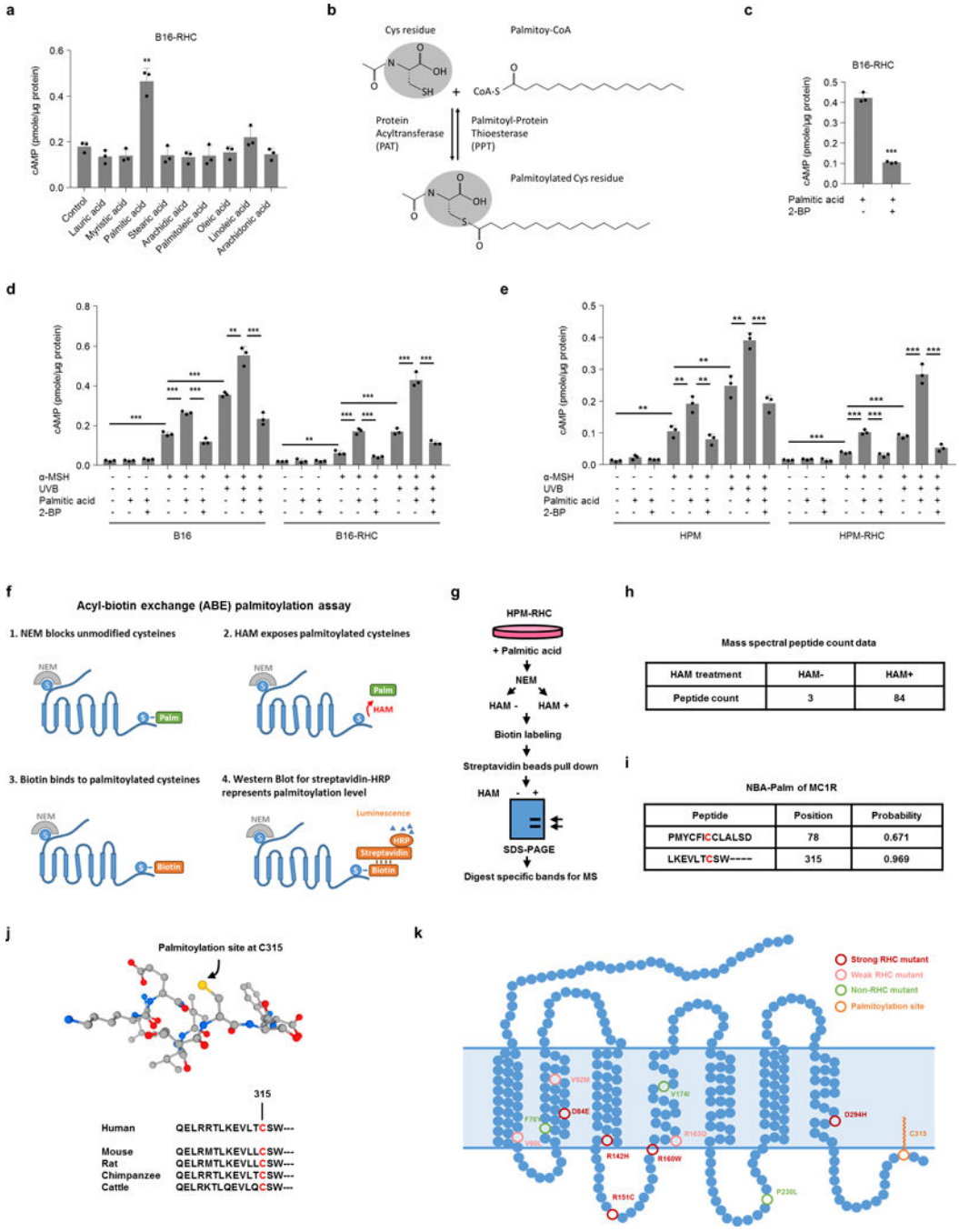

Extended Data Figure 1. MC1R is palmitoylated

(a) Fatty acids were dissolved in 100% ethanol (250 mM) mixed with 25 mM BSA and then added to serum-free DMEM/medium 254 at a final concertation of 500 μM. MC1R RHC-variant B16 cells were serum starved for 6 h. For the last 30 min cells were incubated with 1 μM α-MSH, followed by 100 J/m^2 UVB treatment. Lastly cells were treated with indicated

BSA-conjugated fatty acid medium for 3 h. Results were calculated as mean ± SD from three independent experiments (n=3).

(b) A schematic showing the general process of protein palmitoylation.

(c) MC1R RHC-variant B16 melanoma cells were treated as indicated in (a). 2-BP (25 μM) was added or not with palmitic acid for 3 h and cAMP content was determined. Results were calculated as mean ± SD from three independent experiments (n=3).

(d-e) MC1R RHC-variant or WT B16 melanoma cells (d) and MC1R RHC-variant or WT HPMs (e) were treated as indicated in Figure 1a. 2-BP (25 μM) was added or not with palmitic acid for 3 h and cAMP content was determined. Results were calculated as mean ± SD from three independent experiments (n=3).

(f) A schematic showing the general process of the acyl-biotin exchange (ABE) palmitoylation assay. Unmodified cysteines were irreversibly blocked by N-Ethylmaliemide (NEM), and palmitoylated cysteines were then exposed using HAM and sequentially biotinylated. Biotin levels were determined as a measurement for palmitoylation.

(g) Flowchart of palmitoylated protein identification. NEM, N-Ethylmaleimide. HAM, hydroxylamine. 1×10^8 MC1R RHC-variant HPMs were treated with palmitic acid as indicated in (a), and then processed as shown in flowchart. Streptavidin IP was performed and protein samples were separated by SDS-PAGE before staining by Coomassie brilliant blue. Palmitoylation-specific bands were excised for Mass Spectrometry for protein identification.

(h) The peptide spectral counts of MC1R from Figure 1c.

(i) NBA-palm of MC1R. The prediction shows two possible sites of MC1R palmitoylation.

(j) A schematic illustration showing the palmitoylation site at MC1R C315 predicted by NBA-PALM and PEP-FOLD3, and a schematic showing the conserved C-terminal domain of MC1R.

(k) Membrane topology of MC1R with indicated RHC, non-RHC and palmitoylation site mutants.

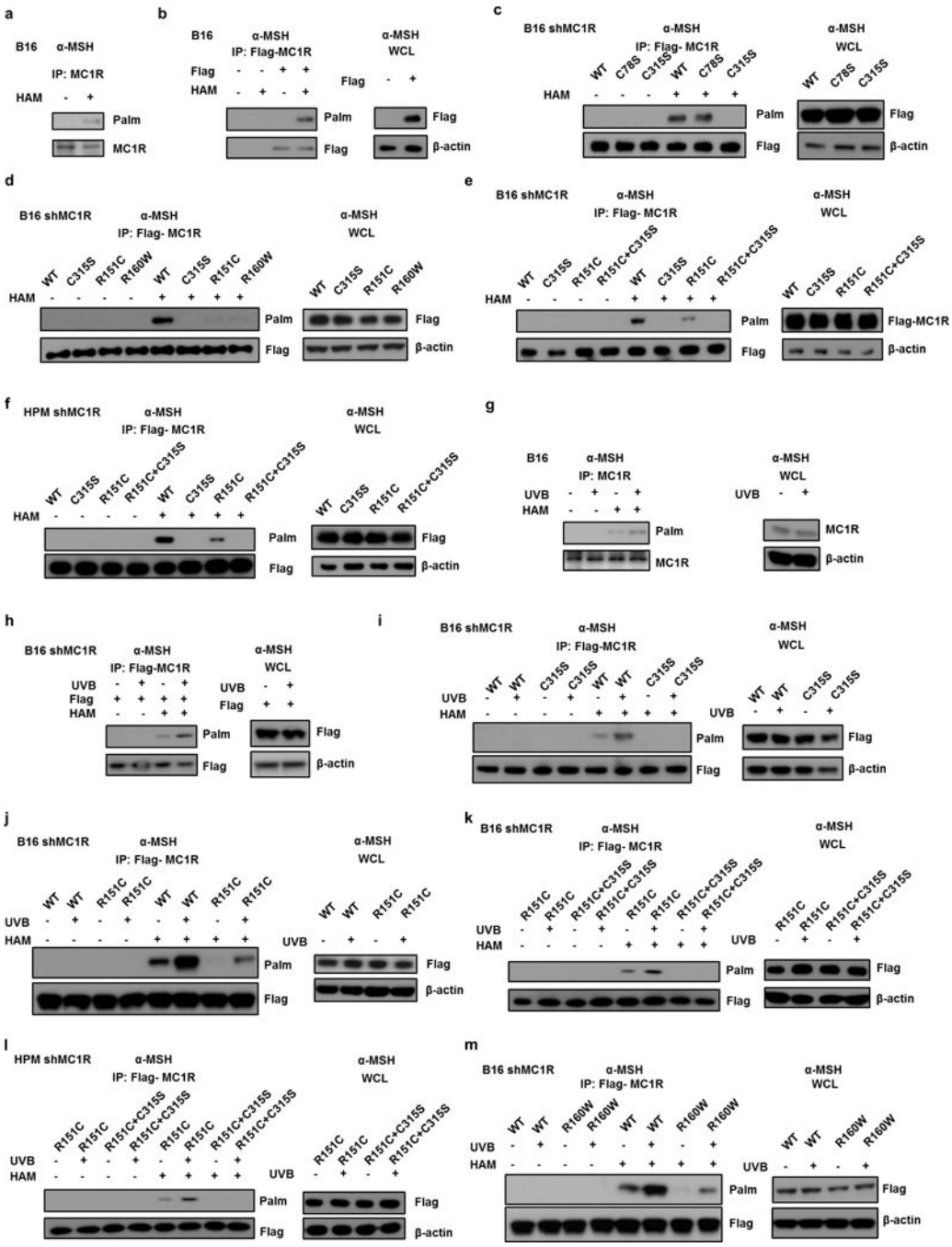

Extended Data Figure 2. Palmitoylation of MC1R in melanocytes

(a) Endogenous MC1R protein is palmitoylated. B16 cells were incubated with 1 μM α-MSH for 3.5 h. Cells were then harvested for IP by specific anti-MC1R antibody, and then for ABE and IB analysis.

(b) Exogenous MC1R protein is palmitoylated. B16 cells were infected with retrovirus encoding Flag-MC1R WT and incubated with 1 μM α-MSH for 3.5 h. Cells were then harvested for IP, ABE and IB analysis.

(c) MC1R is palmitoylated at C315. B16 cells with stable depletion of endogenous MC1R by shRNA were infected with the indicated Flag-MC1R encoding retroviral constructs. Cells were treated with 1 μM α-MSH for 3.5 h and then harvested for IP, ABE and IB analysis.
(d) MC1R RHC variants are defective in palmitoylation. B16 cells with stable depletion of endogenous MC1R by shRNA were infected with the indicated Flag-MC1R encoding retroviral constructs. Cells were treated with 1 μM α-MSH for 3.5 h and then harvested for IP, ABE and IB analysis.
(e-f) R151C does not create a palmitoylation site. B16 cells (e) or HPMs (f) with stable depletion of endogenous MC1R by shRNA were infected with the indicated Flag-MC1R encoding retroviral constructs. Cells were treated with 1 μM α-MSH for 3.5 h and then harvested for IP, ABE and IB analysis.
(g) UVB enhances MC1R palmitoylation. B16 cells were incubated with 1 μM α-MSH for 30 min followed by 100 J/m^2 UVB irradiation. Cells were harvested for IP by specific anti-MC1R antibody, then for ABE and IB analysis 3 h after UVB exposure.
(h) UVB irradiation enhances MC1R palmitoylation. B16 cells were infected with retroviral constructs encoding Flag-MC1R WT and pre-treated with 1 μM α-MSH for 30 min followed by 100 J/m^2 UVB irradiation. Cells were harvested for IP, ABE and IB analysis 3 h after UVB exposure.
(i) MC1R C315S mutant does not respond to UVB irradiation. B16 with stable depletion of MC1R by shRNA were infected with the indicated Flag-MC1R encoding retroviral constructs. Cells were pre-treated with 1 μM α-MSH for 30 min followed by 100 J/m^2 UVB irradiation. Cells were harvested for IP, ABE and IB analysis 3 h after UVB exposure.
(j-m) MC1R RHC variants are defective in palmitoylation after UVB. B16 or HPMs with stable depletion of MC1R by shRNA were infected with the indicated Flag-MC1R encoding retroviral constructs. Cells were pre-treated with 1 μM α-MSH for 30 min followed by 100 J/m^2 UVB irradiation. Cells were harvested for IP, ABE and IB analysis 3 h after UVB exposure.

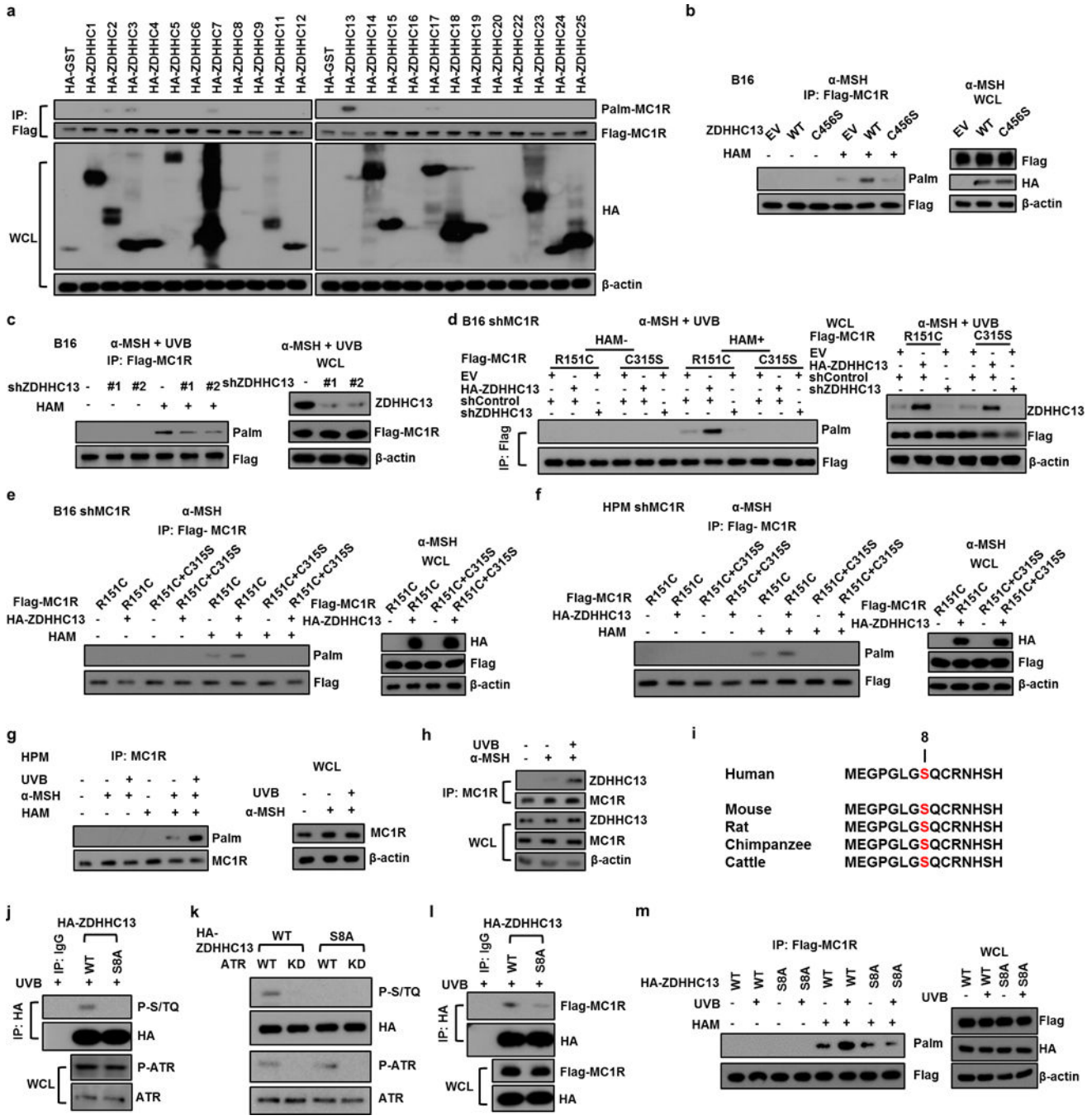

Extended Data Figure 3. ZDHHC13 is a major PAT of MC1R

(a) HEK293 cells were co-transfected with constructs encoding Flag-MC1R and HA-ZDHHCs in 6-well plate. Cells lysates were harvested for IP by anti-Flag antibody, and then for ABE and IB analysis. IB for total MC1R and HA-ZDHHC proteins was shown.

(b) B16 cells were infected with Flag-MC1R and indicated ZDHHC13 WT or C456S mutant encoding retroviral constructs. Cells were treated with 1 μM α-MSH for 3.5 h and then harvested for IP, ABE and IB analysis.

(c) B16 cells with deletion of ZDHHC13 by selective shRNAs were pre-treated with 1 μM α-MSH for 30 min followed by 100 J/m^2 UVB irradiation and harvested for IP, ABE and IB analysis 3 h after UVB exposure.

(d) B16 cells with stable depletion of MC1R by shRNA were infected with the indicated Flag-MC1R encoding retroviral constructs, then cells were infected with shZDHHC13 and/or WT HA-ZDHHC13 expressing virus. Finally, cells were pre-treated with 1 μM α-MSH for 30 min followed by 100 J/m^2 UVB irradiation and harvested for IP, ABE and IB analysis 3 h after UVB exposure.

(e-f) B16 cells or HPMs with stable depletion of MC1R by shRNA were infected with the Flag-MC1R R151C or R151C+C315S double mutant encoding retroviral constructs, then cells were infected with WT HA-ZDHHC13 expressing virus. Finally, cells were pre-treated with 1 μM α-MSH for 3.5 h and harvested for IP, ABE and IB analysis.

(g) HPMs were incubated with 1 μM α-MSH or vehicle for 30 min followed by 100 J/m^2 UVB irradiation. Cells were harvested for IP by specific anti-MC1R antibody, then for ABE and IB analysis 3 h after UVB exposure.

(h) HPMs were incubated with 1 μM α-MSH or vehicle for 30 min followed by 100 J/m^2 UVB irradiation. Cells were harvested for IP by specific anti-MC1R antibody, then for IB analysis 3 h after UVB exposure.

(i) A schematic showing the conserved SQ motif of ZDHHC13.

(j) HPMs were infected with WT ZDHHC13 or ZDHHC13 S8A mutant encoding retroviral constructs, then cells were irradiated with 100 J/m^2 UVB irradiation and harvested for IP and IB analysis 3 h after UVB exposure.

(k) WT Flag-ATR or the kinase-dead (KD) Flag-ATR mutant transfected HEK293 cells were irradiated before Flag beads immunoprecipitation. Then immunoprecipitated WT ZDHHC13 or S8A mutant were incubated with immunoprecipitated WT ATR or the KD ATR mutant in kinase buffer. After reaction, proteins were collected for IB analysis.

(l) HPMs were infected with WT ZDHHC13 or ZDHHC13 S8A mutant and Flag-MC1R encoding retroviral constructs, then cells were irradiated with 100 J/m^2 UVB irradiation and harvested for IP and IB analysis 3 h after UVB exposure.

(m) HPMs cells with stable depletion of ZDHHC13 by shRNA were infected with the indicated ZDHHC13 and Flag-MC1R encoding retroviral constructs. Then cells were pre-treated with 1 μM α-MSH for 30 min followed by 100 J/m^2 UVB irradiation and harvested for IP, ABE and IB analysis 3 h after UVB exposure.

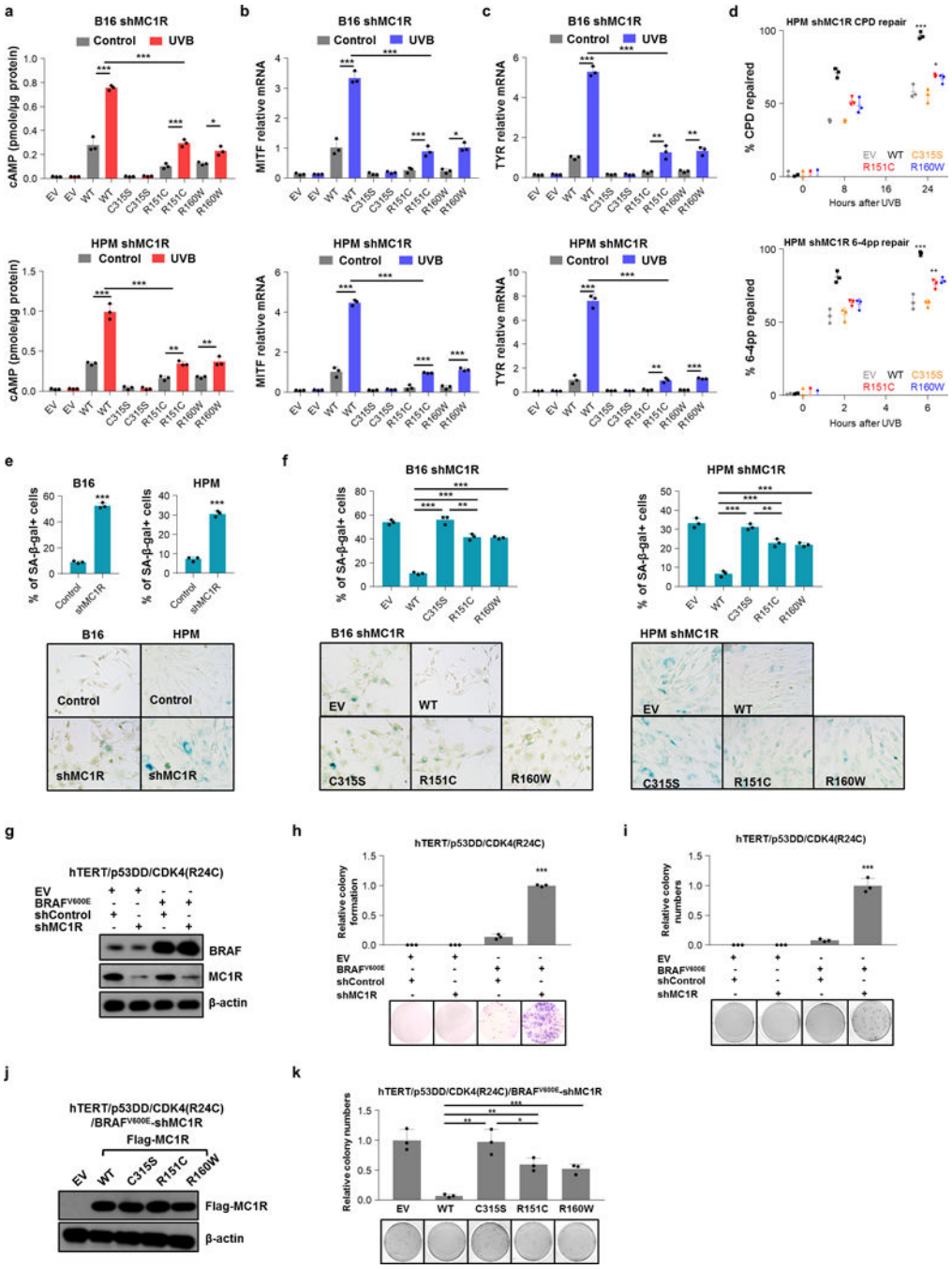

Extended Data Figure 4. Palmitoylation is essential for MC1R function

(a) B16 and HPMs with stable depletion of MC1R by shRNA were infected with the indicated Flag-MC1R encoding retroviral constructs. After 3 h, cells were pre-treated with 1 μM α-MSH for 30 min followed by 100 J/m^2 UVB irradiation. Cells were harvested for a cAMP immunoassay. These data were compiled from three independent experiments. Data are represented as mean ± SD.

(b-c) B16 and HPMs with stable depletion of MC1R by shRNA were infected with the indicated Flag-MC1R encoding retroviral constructs. After 3 h, cells were pre-treated with 1

μM α-MSH for 30 min followed by 100 J/m^2 UVB irradiation. Total RNA were collected for reverse transcription and cDNA were then used for quantitative real time PCR (qRT-PCR) by specific primers targeting mouse/human MITF or TYR. Three independent experiments were quantified. Data are represented as mean ± SD.

(d) HPMs with stable deletion of MC1R by shRNA were infected with the indicated Flag-MC1R encoding retro-viral constructs. Cells were pre-treated with 1 μM α-MSH for 30 min followed by 100 J/m^2 UVB irradiation. Genomic DNA were extracted at the different time points as indicated and photoproducts were detected by ELISA. Cyclobutane pyrimidine dimer (CPD) or 6–4 pyrimidine photoproduct (6–4PP) antibodies were used. Three independent experiments were measured and calculated as mean ± SD.

(e) B16 and HPMs with stable depletion of MC1R by shRNA were pre-treated with 1 μM α-MSH for 30 min followed by 25 J/m^2 UVB irradiation. Cells were subjected to SA-β-gal staining assay 7 days after UVR. The quantification of the percentage of SA-β-gal positive cells and representative pictures were shown. Data shown correspond to one representative experiment out of three independent experiments. Data are represented as mean ± SD.

(f) B16 and HPMs with stable depletion of MC1R by shRNA were infected with the indicated Flag-MC1R encoding retroviral constructs. Cells were pre-treated with 1 μM α-MSH for 30 min followed by 25 J/m^2 UVB irradiation. Cells were subjected to SA-β-gal staining assay 7 days after UVR. The quantification of the percentage of SA-β-gal positive cells and representative pictures were shown. Data shown correspond to one representative experiment out of three independent experiments. Data are represented as mean ± SD.

(g) hTERT/p53DD/CDK4(R24C)/BRAF^{V600E} melanocytes with stable depletion of MC1R by shRNA were pre-incubated with 1 μM α-MSH for 30 min before being irradiated with 20 J/m^2 UVB. Cell lysates were collected for IB analysis.

(h) Cells generated in (g) were subjected to clonogenic survival assays 15 days after UVR. Crystal violet was used to stain colonies and the colony numbers were counted from three independent experiments. The relative colony numbers were calculated as mean ± SD.

(i) Cells generated in (g) were seeded (10,000 cells per well) in 0.5% low-melting-point agarose in DMEM with 10% FBS, layered onto 0.8% agarose in DMEM with 10% FBS. The plates were cultured for 30 days where upon the colonies >50 μm were counted under a light microscope. The colony numbers were plotted as mean ± SD from three independent experiments.

(j) MC1R-depleted hTERT/p53DD/CDK4(R24C)/BRAF^{V600E} melanocytes were further infected with the indicated Flag-MC1R encoding retroviral constructs. Cells were pre-incubated with 1 μM α-MSH for 30min before being irradiated with 20 J/m^2 UVB. Cell lysates were collected for IB analysis.

(k) The cells generated as indicated were seeded (10,000 cells per well) in 0.5% low-melting-point agarose in DMEM with 10% FBS, layered onto 0.8% agarose in DMEM+10% FBS. The plates were cultured for 30 days where upon the colonies >50 μm were counted under a light microscope. The colony numbers were plotted as mean ± SD from three independent experiments.

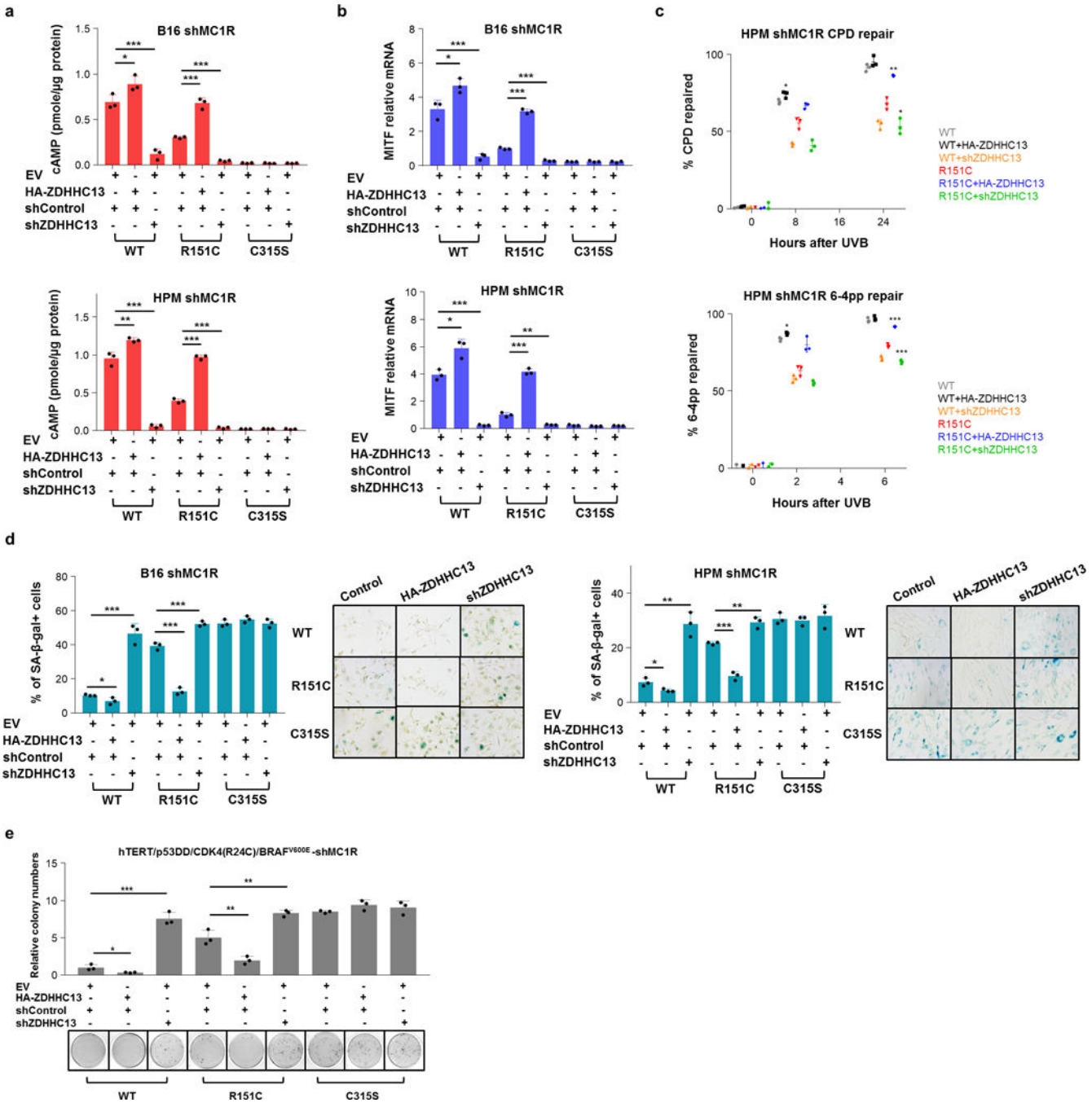

Extended Data Figure 5. Activating MC1R palmitoylation rescues the defect of MC1R RHC variants

(a) B16 and HPMs with stable depletion of MC1R by shRNA were infected with the indicated Flag-MC1R encoding retroviral constructs, then cells were infected with shZDHHC13 and/or WT HA-ZDHHC13 virus. Cells were pre-treated with 1 μM α-MSH for 30 min followed by 100 J/m^2 UVB irradiation. After 3 h, cells were harvested for cAMP immunoassay. These data were compiled from three independent experiments. Data are represented as mean ± SD.

(b) B16 and HPMs with stable depletion of MC1R by shRNA were infected with the indicated Flag-MC1R encoding retroviral constructs, then cells were infected with shZDHHC13 and/or WT HA-ZDHHC13 virus. Cells were pre-treated with 1 μM α-MSH for 30 min followed by 100 J/m^2 UVB irradiation. After 3 h, total RNA was collected for reverse transcription and cDNA were then used for qRT-PCR by specific primers targeting mouse MITF. Three independent experiments were quantified. Data are represented as mean ± SD.

(c) HPMs with stable depletion of MC1R by shRNA were infected with the indicated Flag-MC1R encoding retro-viral constructs, then cells were infected with shZDHHC13 and/or WT HA-ZDHHC13 virus. Cells were pre-treated with 1 μM α-MSH for 30 min followed by 100J/m^2 UVB irradiation. Genomic DNA was extracted at the different time points indicated and photoproducts detected by ELISA using Cyclobutane pyrimidine dimer (CPD) or 6–4 pyrimidine photoproduct (6–4PP) antibodies. Three independent experiments were measured and calculated as mean ± SD.

(d) B16 and HPMs with stable depletion of MC1R by shRNA were infected with the indicated Flag-MC1R encoding retroviral constructs, then cells were infected with shZDHHC13 and/or WT HA-ZDHHC13 virus. Cells were pre-treated with 1 μM α-MSH for 30 min followed by 25 J/m^2 UVB irradiation. Cells were subjected to SA-β-gal staining assay 7 days after UVR. The quantification of the percentage of SA-β-gal positive cells and representative pictures were shown. Data shown correspond to one representative experiment out of three independent experiments. Data are represented as mean ± SD.

(e) The cells generated as indicated were seeded (10,000 cells per well) in 0.5% low-melting-point agarose in DMEM with 10% FBS, layered onto 0.8% agarose in DMEM+10% FBS. Plates were cultured for 30 days where upon the colonies >50 μm were counted under a light microscope. Colony numbers were plotted as mean ± SD from three independent experiments.

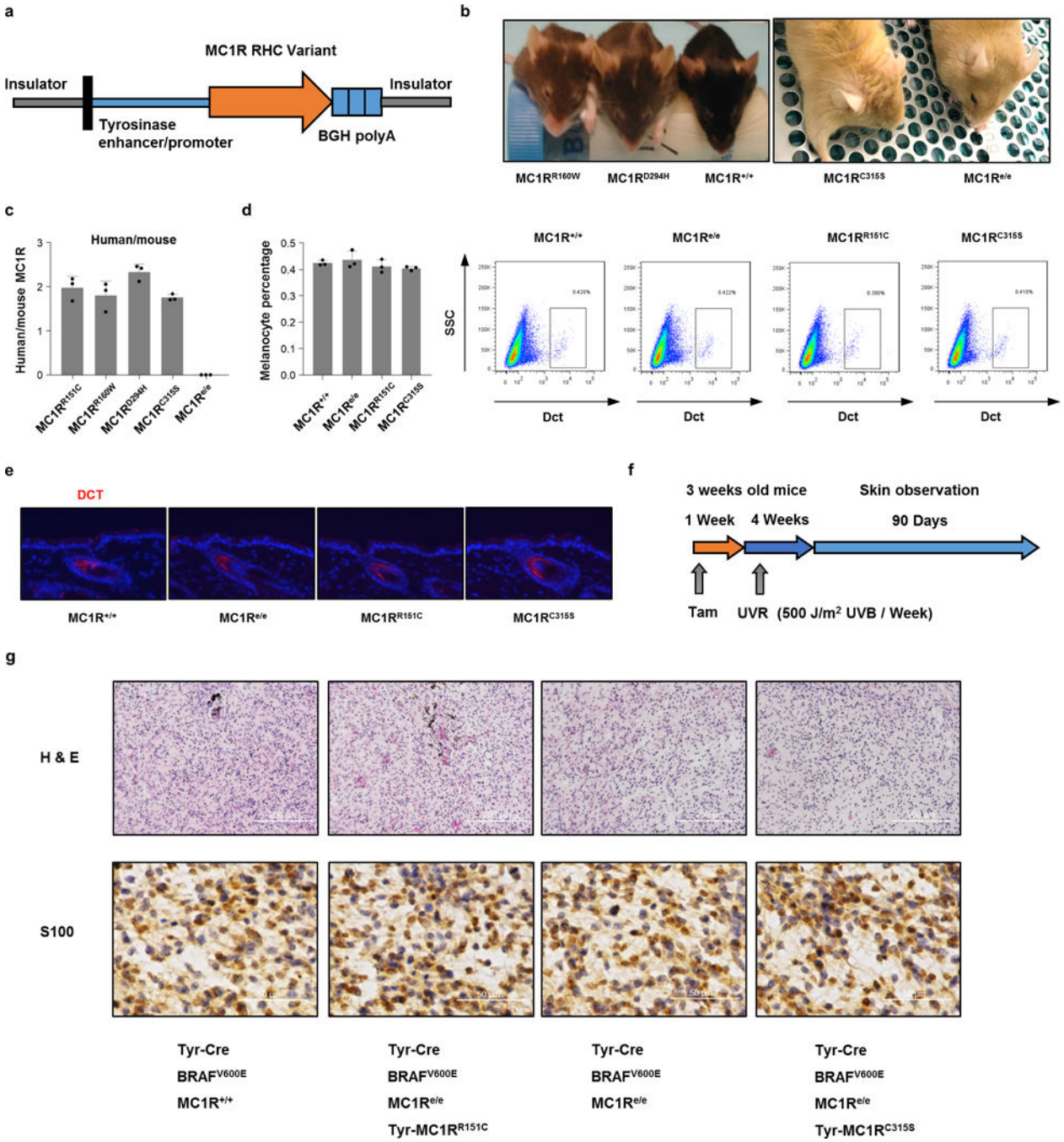

Extended Data Figure 6. MC1R variant and mutant transgenic mice

(a) Schematic diagrams of MC1R variant constructs. Transgenic mice were designed to express melanocyte-specific MC1R variants or mutants (controlled by the Tyr enhancer/promoter).

(b) C57BL/6 MC1R variant or mutant transgenic mice.

(c) Human transgene content in transgenic and control mice. Results were calculated as mean ± SD from three independent experiments.

(d) Whole skins from C57BL/6 MC1R variant transgenic mice (8-12 weeks) were collected and stained with Dct antibody. Melanocytes were then isolated and quantified by FACS sorting. Results were calculated as mean ± SD from three independent experiments.
(e) Frozen sections of skins from C57BL/6 MC1R variant transgenic mice (8-12 weeks) were stained with Dct antibody. The positive staining represents melanocytes.
(f) Illustrations for UVB-induced melanoma development in Tyr-Cre-BRAF^{CA}-MC1R variant mice.
(g) H&E staining of histological sections and immunohistochemistry staining of S100 of representative cutaneous melanomas. Genotypes were showed as indicated.

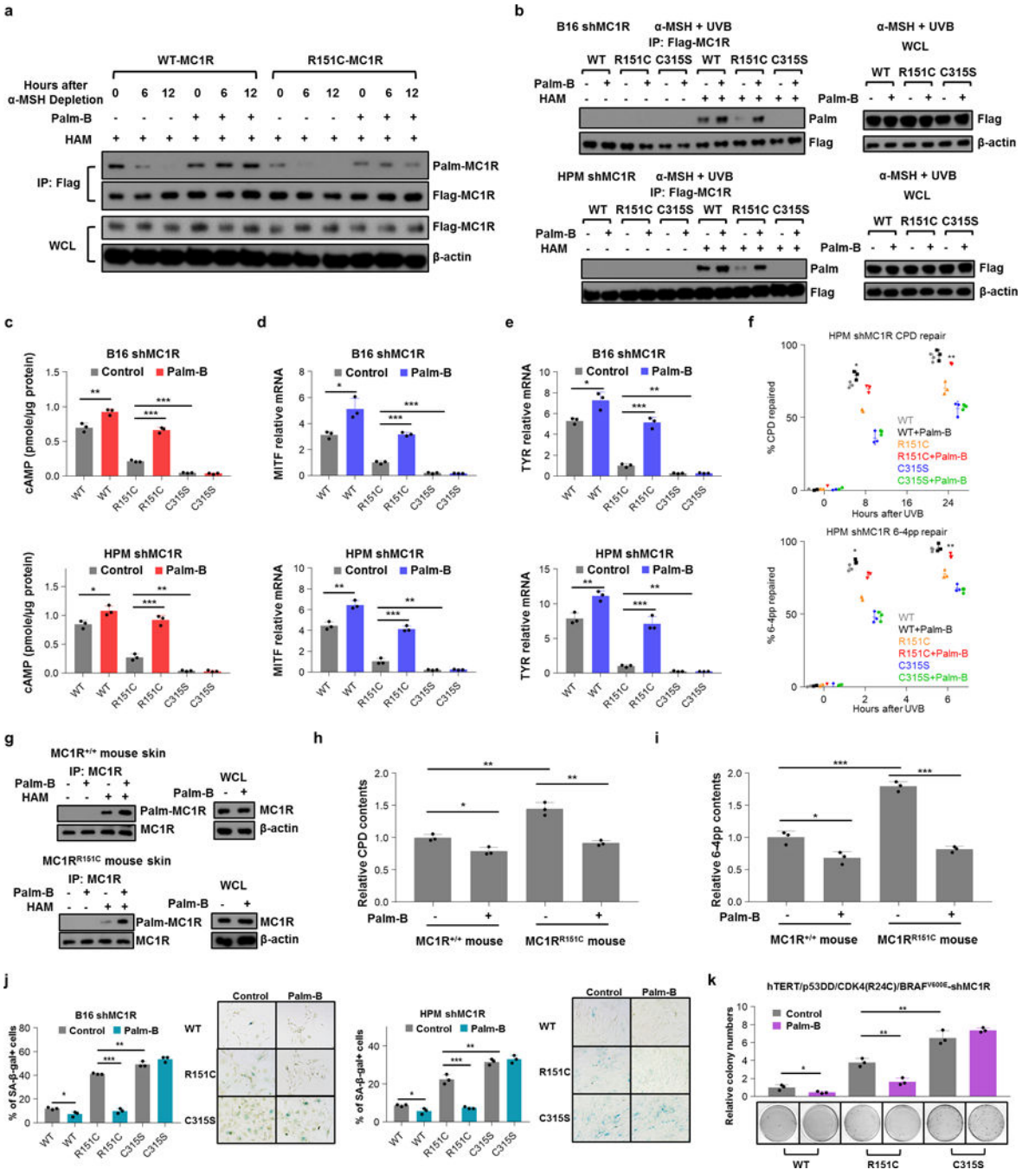

Extended Data Figure 7. Palm-B activates MC1R palmitoylation and rescues the defect of MC1R RHC variants

(a) HPMs were infected with retrovirus encoding Flag-MC1R WT and incubated with 1 μM α-MSH for 3.5 h. The medium was replaced with fresh medium with vehicle or 1 μM Palm-B and cells were treated with indicated time. Cells were harvested for IP, ABE and IB analysis.

(b) B16 and HPMs with stable depletion of MC1R by shRNA were infected with the indicated Flag-MC1R encoding retroviral constructs. Cells were pre-treated with 1 μM α-

MSH and 1 μM Palm-B for 30 min followed by 100 J/m^2 UVB irradiation. Cells were harvested for IP, ABE and IB analysis 3 h after UVB exposure.

(c) B16 and HPMs with stable depletion of MC1R by shRNA were infected with the indicated Flag-MC1R encoding retroviral constructs. Cells were pre-treated with 1 μM α-MSH and 1 μM Palm-B for 30 min followed by 100 J/m^2 UVB irradiation. After 3 h, cells were harvested for cAMP immunoassay. These data were compiled from three independent experiments. Data are represented as mean ± SD.

(d-e) B16 and HPMs with stable depletion of MC1R by shRNA were infected with the indicated Flag-MC1R encoding retroviral constructs. Cells were pre-treated with 1 μM α-MSH and 1 μM Palm-B for 30 min followed by 100 J/m^2 UVB irradiation. After 3 h, total RNA were collected for reverse transcription and cDNA were then used for qRT-PCR by specific primers targeting mouse and/or human MITF or TYR. Three independent experiments were quantified. Data are represented as mean ± SD.

(f) HPMs with stable depletion of MC1R by shRNA were infected with the indicated Flag-MC1R encoding retro-viral constructs. Cells were pre-treated with 1 μM α-MSH and 1 μM Palm-B for 30 min followed by 100 J/m^2 UVB irradiation. Genomic DNA were extracted at the different time points indicated and photoproducts were detected by ELISA. Cyclobutane pyrimidine dimer (CPD) or 6–4 pyrimidine photoproduct (6–4PP) antibodies were used. Three independent experiments were measured and calculated as mean ± SD.

(g) C57BL/6 mice or C57BL/6-MC1R$^{e/e}$-MC1R^{R151C}-tg mice were given a 10 mg/kg Palm-B or vehicle injection intraperitoneally 3 h before UVB irradiation (500 J/m^2). 3 h after UVB, whole skins were collected and the lysates were subjected for IP, ABE and IB analysis.

(h-i) C57BL/6 mice or C57BL/6-MC1R$^{e/e}$-MC1R^{R151C}-tg mouse were injected intraperitoneally with 10 mg/kg Palm-B 3 h before UVB irradiation (500 J/m^2). Melanocytes were isolated by flow cytometry, then DNA were extracted and subjected to ELISA 3 h after UVB irradiation. Results were calculated as mean ± SD from three independent experiments.

(j) B16 with stable depletion of MC1R by shRNA were infected with the indicated Flag-MC1R encoding retroviral constructs. Cells were pre-treated with 1 μM α-MSH and 1 μM Palm-B for 30 min followed by 25 J/m^2 UVB irradiation. Cells were subjected to SA-β-gal staining assay 7 days after UVR. The quantification of the percentage of SA-β-gal positive cells and representative pictures are shown. Data shown correspond to one representative experiment out of three independent experiments. Data are represented as mean ± SD.

(k) The cells generated as indicated were seeded (10,000 cells per well) in 0.5% low-melting-point agarose in DMEM with 10% FBS, layered onto 0.8% agarose in DMEM+10% FBS. The plates were cultured for 30 days where upon the colonies >50 μm were counted under a light microscope. Colony numbers were plotted as mean ± SD from three independent experiments.

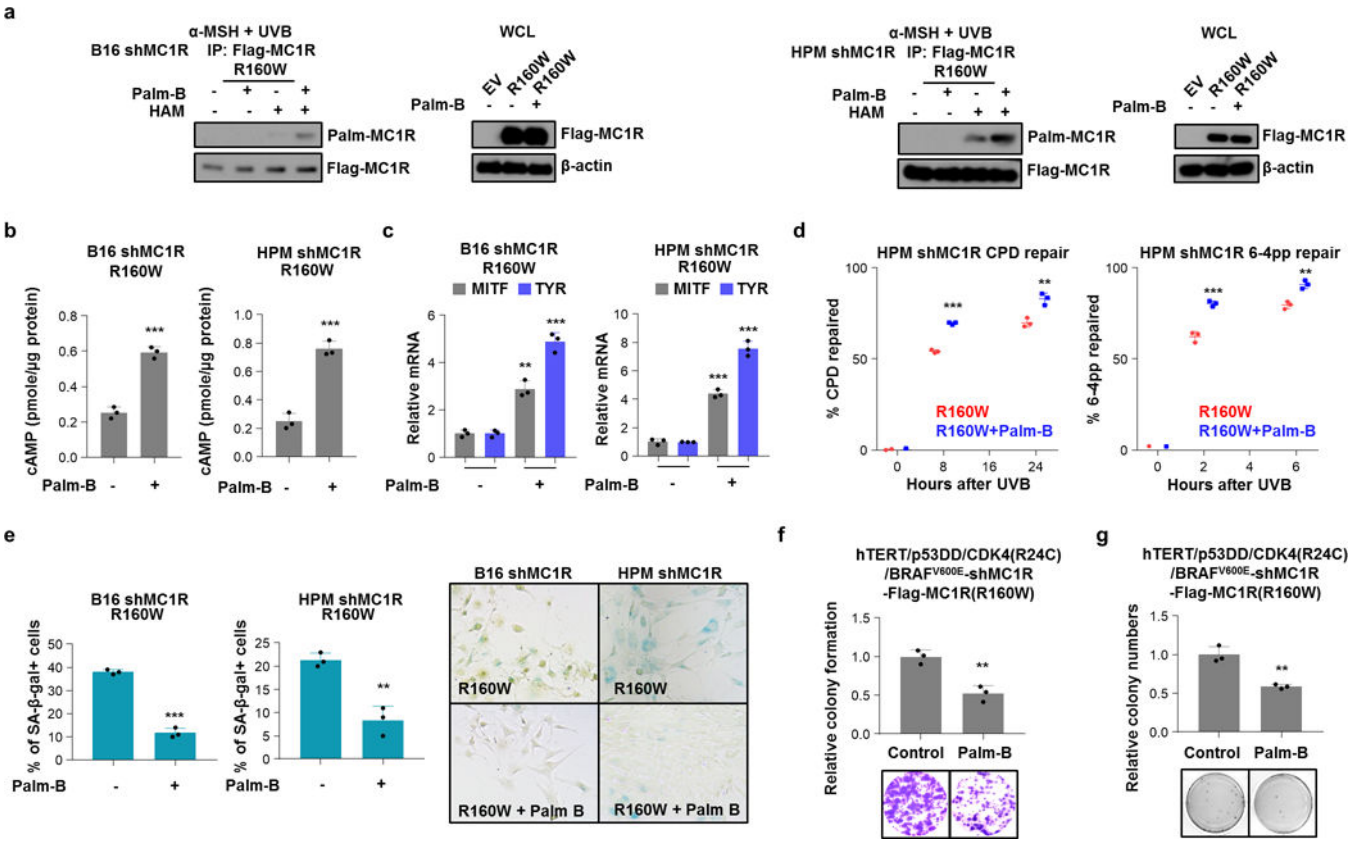

Extended Data Figure 8. Palm-B rescues the defect of MC1R R160W variant

(a) B16 and HPMs with stable depletion of MC1R by shRNA were infected with the indicated Flag-MC1R encoding retroviral constructs. Cells were pre-treated with 1 μM α-MSH and 1 μM Palm-B for 30 min followed by 100 J/m^2 UVB irradiation. Cells were harvested for IP, ABE and IB analysis at 3 h after UVB exposure.

(b) B16 and HPMs with stable depletion of MC1R by shRNA were infected with the indicated Flag-MC1R encoding retroviral constructs. Cells were pre-treated with 1 μM α-MSH and 1 μM Palm-B for 30 min followed by 100 J/m^2 UVB irradiation. After 3 h, cells were harvested for cAMP immunoassay. These data were compiled from three independent experiments. Data are represented as mean ± SD.

(c) B16 and HPMs with stable depletion of MC1R by shRNA were infected with the indicated Flag-MC1R encoding retroviral constructs. Cells were pre-treated with 1 μM α-MSH and 1 μM Palm-B for 30 min followed by 100 J/m^2 UVB irradiation. After 3 h, total RNA was collected for reverse transcription and cDNA then used for qRT-PCR by specific primers targeting mouse and/or human MITF or TYR. Three independent experiments were quantified. Data are represented as mean ± SD.

(d) HPMs with stable depletion of MC1R by shRNA were infected with the indicated Flag-MC1R encoding retroviral constructs. Cells were pre-treated with 1 μM α-MSH and 1 μM Palm-B for 30 min followed by 100 J/m^2 UVB irradiation. Genomic DNA were extracted at the different time points indicated and photoproducts were detected by ELISA using anti-cyclobutane pyrimidine dimer (CPD) or 6–4 pyrimidine photoproduct (6–4PP) antibodies. Three independent experiments were measured and calculated as mean ± SD.

(e) B16 and HPMs with stable depletion of MC1R by shRNA were infected with the indicated Flag-MC1R encoding retroviral constructs. Cells were pre-treated with 1 μM α-MSH and 1 μM Palm-B for 30 min followed by 25 J/m^2 UVB irradiation. Cells were subjected to SA-β-gal staining assay 7 days after UVR. The quantification of the percentage of SA-β-gal positive cells and representative pictures are shown and correspond to one representative experiment out of three independent experiments. Data are represented as mean ± SD.

(f) MC1R-depleted hTERT/p53DD/CDK4(R24C)/$BRAF^{V600E}$ melanocytes were further infected with the indicated Flag-MC1R encoding retro-viral constructs. Cells were pre-incubated with 1 μM α-MSH and 1 μM Palm-B for 30min before being irradiated with 20 J/m^2 UVB, and then subjected to clonogenic survival assays 15 days after UVR. Crystal violet was used to stain colonies and the colony numbers were counted from three independent experiments. The relative colony numbers were calculated as mean ± SD.

(g) The cells generated in (k) were seeded (10,000 cells per well) in 0.5% low-melting-point agarose in DMEM with 10% FBS, layered onto 0.8% agarose in DMEM+10% FBS. Plates were cultured for 30 days where upon the colonies >50 μm were counted under a light microscope. The colony numbers were plotted as mean ± SD from three independent experiments.

Supplementary Material

Refer to Web version on PubMed Central for supplementary material.

Acknowledgments

We thank Drs. Xuebiao Yao, Huafeng Xie and Guo Wei for careful reading and suggestions. This work was supported by the National Institutes of Health (RC: R01CA137098, R01CA193913 and R01CA196896), Department of Defense (RC: CA140020), Melanoma Research Foundation Establish Investigator Award (RC), Hong Kong and Macao Young Scientists of the National Natural Science Foundation of China (RC: 81428025), National Natural Science Foundation of China (XG: 81630106), and the Ludwig Institute for Cancer Research (CRG). RC is American Cancer Society Research Scholar.

References

1. Jackson IJ, Budd PS, Keighren M, McKie L. Humanized MC1R transgenic mice reveal human specific receptor function. Hum Mol Genet. 2007; 16:2341–2348. [PubMed: 17652101]
2. D'Orazio JA, et al. Topical drug rescue strategy and skin protection based on the role of Mc1r in UV-induced tanning. Nature. 2006; 443:340–344. [PubMed: 16988713]
3. Healy E, et al. Functional variation of MC1R alleles from red-haired individuals. Hum Mol Genet. 2001; 10:2397–2402. [PubMed: 11689486]
4. Palmer JS, et al. Melanocortin-1 receptor polymorphisms and risk of melanoma: is the association explained solely by pigmentation phenotype? Am J Hum Genet. 2000; 66:176–186. [PubMed: 10631149]
5. Raimondi S, et al. MC1R variants, melanoma and red hair color phenotype: a meta-analysis. Int J Cancer. 2008; 122:2753–2760. [PubMed: 18366057]
6. Goldstein AM, et al. Association of MC1R variants and risk of melanoma in melanoma-prone families with CDKN2A mutations. Cancer Epidemiol Biomarkers Prev. 2005; 14:2208–2212. [PubMed: 16172233]
7. Landi MT, et al. MC1R, ASIP, and DNA repair in sporadic and familial melanoma in a Mediterranean population. J Natl Cancer Inst. 2005; 97:998–1007. [PubMed: 15998953]

8. Harding RM, et al. Evidence for variable selective pressures at MC1R. Am J Hum Genet. 2000; 66:1351–1361. [PubMed: 10733465]
9. Garcia-Borron JC, Sanchez-Laorden BL, Jimenez-Cervantes C. Melanocortin-1 receptor structure and functional regulation. Pigment Cell Res. 2005; 18:393–410. [PubMed: 16280005]
10. Abdel-Malek ZA, et al. alpha-MSH tripeptide analogs activate the melanocortin 1 receptor and reduce UV-induced DNA damage in human melanocytes. Pigment Cell Melanoma Res. 2009; 22:635–644. [PubMed: 19558415]
11. Bohm M, et al. alpha-Melanocyte-stimulating hormone protects from ultraviolet radiation-induced apoptosis and DNA damage. J Biol Chem. 2005; 280:5795–5802. [PubMed: 15569680]
12. Kadekaro AL, et al. alpha-Melanocortin and endothelin-1 activate antiapoptotic pathways and reduce DNA damage in human melanocytes. Cancer Res. 2005; 65:4292–4299. [PubMed: 15899821]
13. Abdel-Malek ZA, Knittel J, Kadekaro AL, Swope VB, Starner R. The melanocortin 1 receptor and the UV response of human melanocytes–a shift in paradigm. Photochem Photobiol. 2008; 84:501–508. [PubMed: 18282187]
14. Dong L, W J, Zhang X, Pier E, Zhang B, Dong F, Ziegler N, Mysz M, Armenta Z, Cui R. α-Melanocytes-stimulating Hormone, a potential activator of XPA DNA repair. Cancer Res. 2010; 70:3547–3556. [PubMed: 20388774]
15. Robles-Espinoza CD, et al. Germline MC1R status influences somatic mutation burden in melanoma. Nature communications. 2016; 7:12064.
16. Premi S, et al. Photochemistry. Chemiexcitation of melanin derivatives induces DNA photoproducts long after UV exposure. Science. 2015; 347:842–847. [PubMed: 25700512]
17. Kanetsky PA, et al. Does MC1R genotype convey information about melanoma risk beyond risk phenotypes? Cancer. 2010; 116:2416–2428. [PubMed: 20301115]
18. Williams PF, Olsen CM, Hayward NK, Whiteman DC. Melanocortin 1 receptor and risk of cutaneous melanoma: a meta-analysis and estimates of population burden. Int J Cancer. 2011; 129:1730–1740. [PubMed: 21128237]
19. Olsen CM, Carroll HJ, Whiteman DC. Estimating the attributable fraction for melanoma: a meta-analysis of pigmentary characteristics and freckling. Int J Cancer. 2010; 127:2430–2445. [PubMed: 20143394]
20. Cust AE, et al. MC1R genotypes and risk of melanoma before age 40 years: A population-based case-control-family study. Int J Cancer. 2012
21. Xue Y, Chen H, Jin C, Sun Z, Yao X. NBA-Palm: prediction of palmitoylation site implemented in Naive Bayes algorithm. BMC Bioinformatics. 2006; 7:458. doi:1471-2105-7-458. [PubMed: 17044919]
22. Fukata M, Fukata Y, Adesnik H, Nicoll RA, Bredt DS. Identification of PSD-95 palmitoylating enzymes. Neuron. 2004; 44:987–996. [PubMed: 15603741]
23. Hilton BA, et al. ATR Plays a Direct Antiapoptotic Role at Mitochondria, which Is Regulated by Prolyl Isomerase Pin1. Molecular cell. 2015; 60:35–46. [PubMed: 26387736]
24. Cimprich KA, Cortez D. ATR: an essential regulator of genome integrity. Nature reviews. Molecular cell biology. 2008; 9:616–627. [PubMed: 18594563]
25. Cao J, et al. MC1R is a potent regulator of PTEN after UV exposure in melanocytes. Molecular cell. 2013; 51:409–422. [PubMed: 23973372]
26. Garraway LA, et al. Integrative genomic analyses identify MITF as a lineage survival oncogene amplified in malignant melanoma. Nature. 2005; 436:117–122. DOI: 10.1038/nature03664 [PubMed: 16001072]
27. Dankort D, et al. Braf(V600E) cooperates with Pten loss to induce metastatic melanoma. Nat Genet. 2009; 41:544–552. [PubMed: 19282848]
28. Lin DT, Conibear E. ABHD17 proteins are novel protein depalmitoylases that regulate N-Ras palmitate turnover and subcellular localization. Elife. 2015; 4:e11306. [PubMed: 26701913]
29. Dekker FJ, et al. Small-molecule inhibition of APT1 affects Ras localization and signaling. Nature chemical biology. 2010; 6:449–456. [PubMed: 20418879]

30. Cui R, et al. Central role of p53 in the suntan response and pathologic hyperpigmentation. Cell. 2007; 128:853–864. [PubMed: 17350573]
31. Diffey BL, Jansen CT, Urbach F, Wulf HC. The standard erythema dose: a new photobiological concept. Photodermatol Photoimmunol Photomed. 1997; 13:64–66. [PubMed: 9361131]
32. Horikawa T, Norris DA, Zekman T, Morelli JG. Effective elimination of fibroblasts in cultures of melanocytes by lowering calcium concentration in TPA depleted medium following geneticin treatment. Pigment Cell Res. 1996; 9:58–62. [PubMed: 8857666]
33. Dunham WR, Klein SB, Rhodes LM, Marcelo CL. Oleic acid and linoleic acid are the major determinants of changes in keratinocyte plasma membrane viscosity. J Invest Dermatol. 1996; 107:332–335. [PubMed: 8751966]
34. Jiang G, Sancar A. Recruitment of DNA damage checkpoint proteins to damage in transcribed and nontranscribed sequences. Mol Cell Biol. 2006; 26:39–49. [PubMed: 16354678]
35. Wakamatsu K, Ito S. Advanced chemical methods in melanin determination. Pigment Cell Res. 2002; 15:174–183. [PubMed: 12028581]

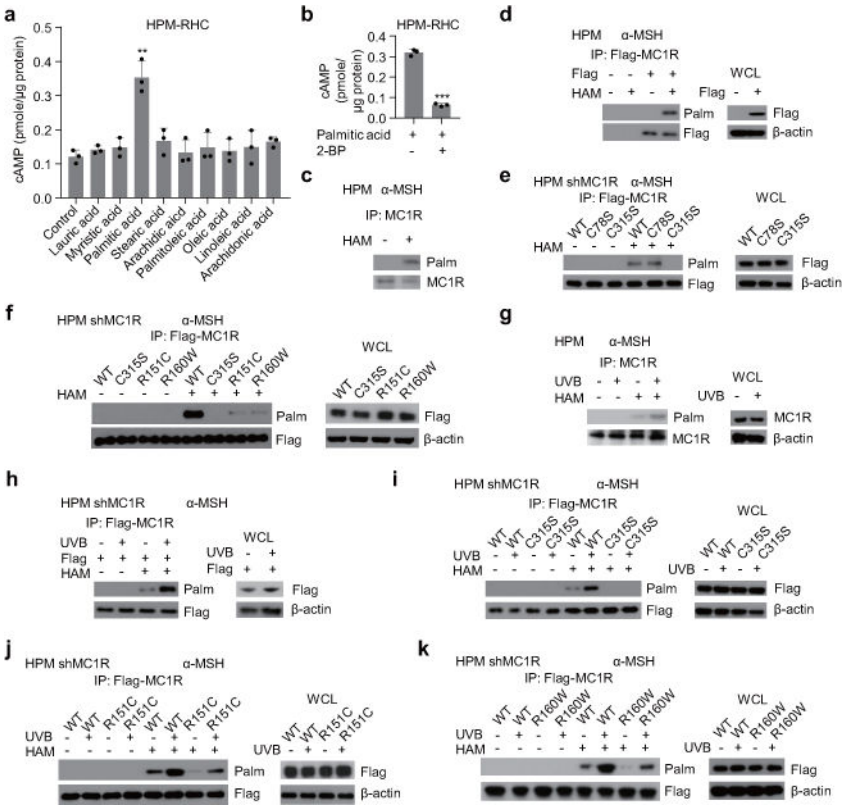

Figure 1. Palmitoylation of MC1R in melanocytes

a-b, MC1R RHC-variant HPMs exposed to α-MSH and UVB irradiated were treated with BSA-conjugated fatty acids. **b**, cells were exposed to palmitic acid +/− 2-BP. cAMP were calculated by three independent experiments shown as mean ± SD. **c-f**, HPMs (**c**), HPMs expressing WT, mutant or variant Flag-MC1R (**d-f**) were incubated with α-MSH and processed for ABE analysis. **g-k**, HPMs (**g**), HPMs expressing WT, mutant or variant Flag-MC1R (**h-k**) were treated with α-MSH, irradiated with UVB, and harvested for ABE analysis. Western blots shown were representative of three independent experiments. **p<0.01, ***p<0.001, unpaired student's t-test. For gel source data, see Supplementary Figure 1.

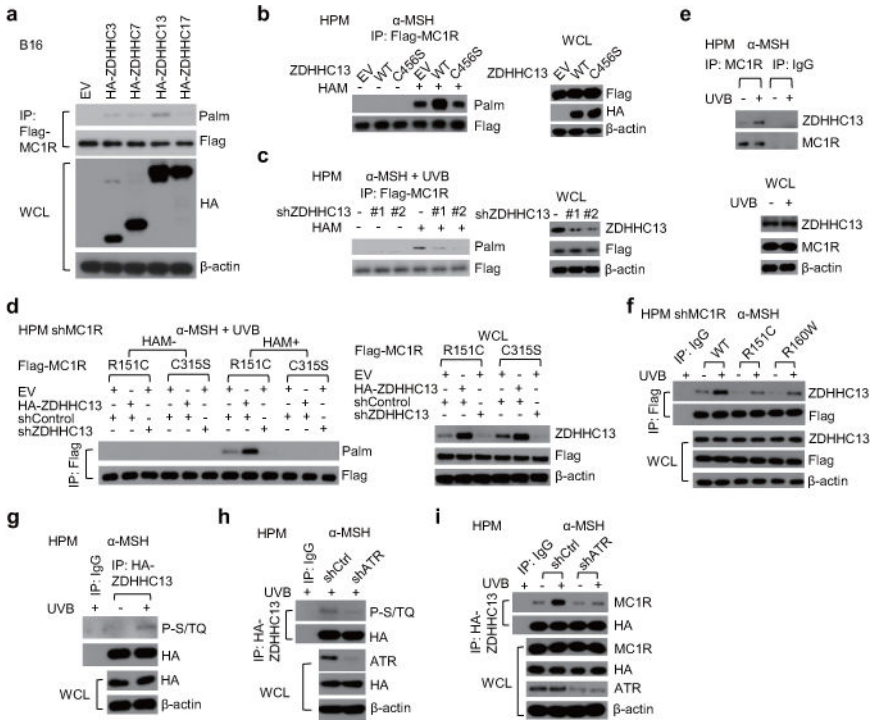

Figure 2. ZDHHC13 is a major MC1R palmitoyl acyltransferase

a-b, B16 cells co-expressing Flag-MC1R and HA-ZDHHCs (**a**) and HPMs expressing Flag-MC1R and ZDHHC13 WT or C456S mutant (**b**) were incubated with α-MSH and processed for ABE analysis. **c-f**, HPMs expressing ZDHHC13 shRNAs (**c**), HPMs expressing Flag-MC1R together with shZDHHC13 and/or WT HA-ZDHHC13 (**d**), HPMs (**e**) and HPMs expressing Flag-MC1R (**f**) were pre-treated with α-MSH, UVB irradiated and harvested for IP, ABE and IB. **g-i**, HPMs expressing HA-ZDHHC13 (**g**), HPMs expressing shATR and HA-ZDHHC13 (**h-i**) were pre-treated with α-MSH, UVB irradiated and processed for IP and IB analysis. Western blots shown were representative of three independent experiments. For gel source data, see Supplementary Figure 1.

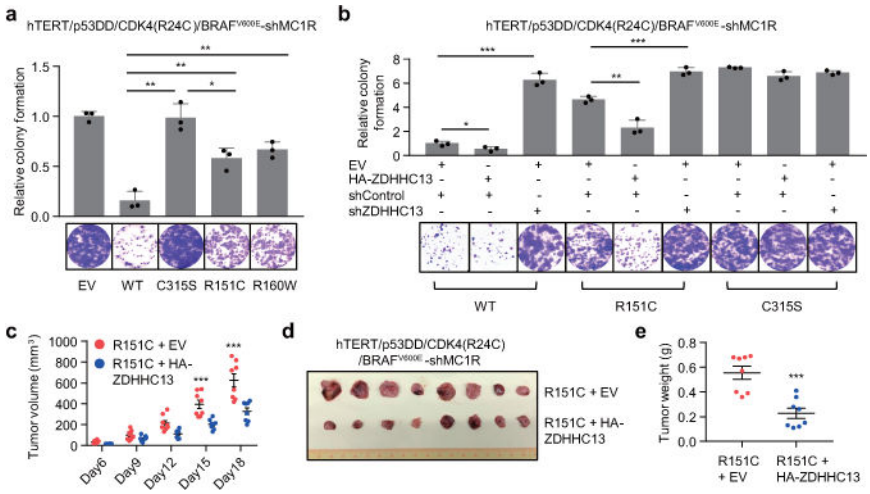

Figure 3. Activating MC1R palmitoylation rescues the defect of MC1R RHC variants

a-b, MC1R-depleted hTERT/p53DD/CDK4(R24C)/BRAF^{V600E} melanocytes expressing Flag-MC1R (**a**) or cells further infected with shZDHHC13 and/or WT HA-ZDHHC13 virus (**b**) were pre-incubated with α-MSH, UVB irradiated and assayed for clonogenic survival. Results were calculated as mean ± SD from three independent experiments. **c-e**, Growth curves (**c**), dissected tumors (**d**) and tumor weight (**e**) for the xenograft experiments with indicated cells inoculated subcutaneously into each flank of nude mice (n=8). Visible tumors were measured at the indicated days. Error bars represent ±SEM. *p<0.05, **p<0.01, ***p<0.001, unpaired student's t-test.

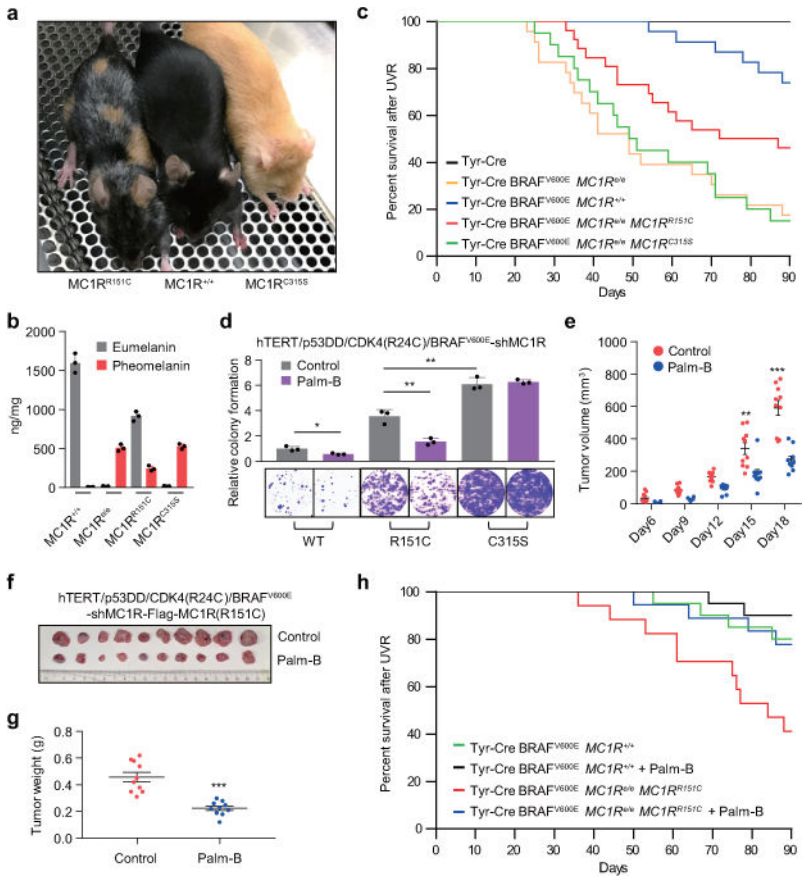

Figure 4. MC1R palmitoylation controls melanomagenesis

a, C57BL/6 MC1R variant transgenic mice. **b**, Eumelanin and pheomelanin content of whole skin from C57BL/6 MC1R variant transgenic mice. Data shown represent the mean ± SD of three independent experiments. **c**, Melanoma-free survival. Tyr-Cre n=15, Tyr-Cre-BRAF^{V600E}-*MC1R$^{e/e}$* n=23, Tyr-Cre-BRAF^{V600E}-*MC1R$^{+/+}$* n=23, Tyr-Cre-BRAF^{V600E}-*MC1R$^{e/e}$*-*MC1R^{R151C}* n=26, Tyr-Cre-BRAF^{V600E}-*MC1R$^{e/e}$*-*MC1R^{C315S}* n=20. By Log-rank test, p=0.0001 (e/e & +/+), p=0.0179 (e/e & R151C), p=0.8943 (e/e & C315S), p=0.0232 (+/+ & R151C), p=0.0001 (+/+ & C315S), p=0.0233 (R151C & C315S). **d**, Indicated melanocytes were treated with α-MSH and Palm-B before UVB irradiation and assayed for clonogenic survival. Results were calculated as mean ± SD from three independent experiments. **e-g**, Growth curves (**e**), dissected tumors (**f**) and tumor weight (**g**) for subcutaneous xenograft experiments in nude mice (n=10) using indicated cells. Error bars represent ±SEM. **h**, Melanoma-free survival of Tyr-Cre-BRAF^{V600E}-*MC1R$^{+/+}$* n=20, Tyr-Cre-BRAF^{V600E}-*MC1R$^{+/+}$* + Palm-B n=20, Tyr-Cre-BRAF^{V600E}-*MC1R$^{e/e}$*-*MC1R^{R151C}* n=17, Tyr-Cre-BRAF^{V600E}-*MC1R$^{e/e}$*-*MC1R^{R151C}* + Palm-B n=18. By Log-rank test, p=0.0241 (R151C & R151C + Palm-B), p=0.3711 (MC1R$^{+/+}$ & MC1R$^{+/+}$ + Palm-B). *p<0.05, **p<0.01, ***p<0.001, unpaired student's t-test.